Aalto University
School of Chemical
Engineering

Victoria Lindqvist

PREPARATION AND CHARACTERIZATION OF A NANOCELLULOSE REINFORCED LIGHT-POLYMERIZED METHACRYLATE-BASED DENTAL ADHESIVE

Master´s Programme in Chemical, Biochemical and Materials Engineering
Major in Fiber and Polymer Engineering

Master's thesis for the degree of Master of Science in Technology submitted for inspection, Espoo, 14.03.2019.

Thesis supervisor Professor Eero Kontturi

Thesis advisors Professor Pekka Vallittu
Ph.D. Katja Heise

Aalto University
School of Chemical
Engineering

Aalto University, P.O. BOX 11000, 00076 AALTO
www.aalto.fi

Abstract of master's thesis

Author Victoria Lindqvist

Title of thesis Preparation and characterization of a nanocellulose reinforced light-polymerized methacrylate-based dental adhesive

Degree Programme Master's programme in Chemical, Biochemical and Materials Engineering

Major Fiber and Polymer Engineering

Thesis supervisor Professor Eero Kontturi

Thesis advisors Professor Pekka Vallittu, Ph.D. Katja Heise

Date 14.03.2019. **Number of pages**: 5+83. **Language:** English.

Abstract

The purpose of this research work was to develop a new dental adhesive, by inclusion of cellulose nanocrystals (CNCs) into a polymer matrix. CNCs were chosen as a component for dental adhesives due to its mechanical properties, dimensions, low density and biocompatibility. Two methacrylate co-monomer mixtures: 2-hydroxyethyl methacrylate (HEMA) and Bisphenol A Glycidyl Methacrylate (bisGMA) were used as model dentin adhesive polymer matrices. In the work, three types of CNCs were prepared by acid hydrolysis, using three acids: sulphuric, phosphoric and hydrochloric acid. In order to improve dispersion of CNCs in methacrylate-based matrices, each type of CNCs was modified. 3-Trimethoxysilyl propyl methacrylate was chosen as a coupling agent able to improve dispersion and co-polymerization of CNCs in methacrylate-based matrices. FTIR and Liquid-State NMR analysis were used to confirm the results of CNCs modification.

Based on evaluation of dispersibility of CNCs and the results of modification, CNCs prepared through phosphoric acid hydrolysis (PCNCs) were found as the most suitable component for the dental adhesive application. Nanocomposite samples were prepared from both matrices and freeze-dried pristine and modified PCNCs with the weight concentration up to 5%. Influence of the incorporated pristine and modified PCNCs on the conversion profile of the experimental nanocomposite was studied. Mechanical properties of the *in situ* light-polymerized nanocomposites were studied by Flexural strength test. TEM was used to investigate nanostructure of the experimental dental adhesives. Real-time FTIR photo-polymerization studies were done to evaluate the effect of PCNCs inclusion on the kinetics of polymerization for the nanocomposites.

The results of mechanical testing showed a slight improvement of flexural strength for the nanocomposite out of HEMA-based resin and 5 wt.% PCNCs, however, modified PCNCs did not improve the strength of the experimental material. For the nanocomposite samples out of bisGMA-based resin PCNCs slightly reduced flexural strength. Study of nanostructure revealed the improved dispersibility of modified PCNCs in the matrix compared to pristine PCNCs. Inclusion of pristine or modified PCNCs did not reduce the degree of conversion of the resulting nanocomposites.

The outcomes of this work demonstrate that PCNCs have a potential to become a valuable component in methacrylate-based polymer matrices. PCNCs could act as reinforcement part for lacking mechanical strength HEMA-based adhesives, while for the strong hydrophobic bisGMA-based matrix PCNCs could increase biocompatibility. However, the current research provides the information for the further studies, and comprehensive research is required.

Keywords: cellulose nanocrystal, dental adhesive, methacrylate, photo-polymerization, nanocomposite, sylilation, phosphoric acid hydrolysis, HEMA, bisGMA, CNC, dentin bonding

Preface

The thesis work has been carried out at the Department of Bioproducts and Biosystems of Aalto University, in cooperation with Turku University Institute of Dentistry and Stick Tech Ltd. I am grateful for the given me opportunity to work in this exciting and challenging novel project.

First, I would like to thank my supervisor Professor Eero Kontturi for all the guidance through up my research project, support, encouragement and knowledge he has given me during this project. I appreciate Ph.D. (Chem) Eija Säilynoja for her very friendly and supportive guidance through this work and Professor Pekka Vallittu for sharing his expertise and experience. I would like to thank my thesis instructor Ph.D. (Chem) Katja Heise for providing practical advises, sharing ideas and given support through the work.

It has been wonderful experience to work in Eero's group with all the team members. I would like to thank especially: Panos Spiliopoulos, Timo Pääkkönen and Iina Solala for the active participation and contribution to the project.

I am grateful to Alistar King and Tetyana Koto, Nonappa and Henna Hallgren for the help in carrying out the research. And, last but not least, I thank Marja Kärkkäinen and Rita Hatakka for their help with practical issues in the laboratory.

In addition, I would like to thank everyone, working and studying in the Bio^2 department, for the creating excellent atmosphere, friendly and relaxed, fully conducive to fruitful research.

Victoria Lindqvist

Otaniemi, 21.01.2019

Contents

Symbols and abbreviations

AFM	Atomic Force Microscopy
bisGMA	Bisphenol A Glycidyl Methacrylate
CNC(s)	cellulose nanocrystal(s)
CQ	(1R)-(−)-Camphorquinone
CVD	Chemical Vapour Deposition
DMAEMA	2-(dimethylamino)ethyl methacrylate
EDMAB	ethyl-4-(dimethylamino) benzoate
FTIR	Fourier trans-form infrared (spectroscopy)
HCNC(s)	cellulose nanocrystal(s) prepared by HCl hydrolysis
HEMA	2-hydroxyethyl methacrylate
HQ	benzene-1,4-diol (hydroquinone)
LED	Light emitting diode
Milli-Q	Deionized water purified with Millipore Synergy UV unit
mPCNC1(s)	modified by Method 1 cellulose nanocrystal(s) isolated by phosphoric acid hydrolysis
mPCNC2(s)	modified by Method 2 cellulose nanocrystal(s) isolated by phosphoric acid hydrolysis
MPS	3-Trimethoxysilyl propyl methacrylate
mSCNC1(s)	modified by Method 1 cellulose nanocrystal(s) isolated by phosphoric acid hydrolysis
mSCNC2(s)	modified by Method 2 cellulose nanocrystal(s) isolated by phosphoric acid hydrolysis
NMR	Nuclear Magnetic Resonance (spectroscopy)
PAS-IR	photoacoustic infrared (spectroscopy)
PCNC(s)	cellulose nanocrystal(s) isolated by phosphoric acid hydrolysis
PHEMA	poly(2-hydroxyethyl methacrylate)
SCNC(s)	cellulose nanocrystal(s) isolated by sulphuric acid hydrolysis
TEGDMA	triethylene glycol dimethactylate
TEM	Transmission Electron Microscopy
UV	ultraviolet
v/v%	volume/volume percent
wt.%	percent by weight

1. Introduction

Cellulose, the most common biopolymer on Earth, has been traditionally widely used by humankind in construction, papermaking, textile and food utilization, mostly in low-added value products and materials. However, during the past century, the fundamental knowledge about cellulose polymer structure, its solubility and chemical modification increased and contributed the appearance of new forms of cellulosic material, such as cellulose derivatives and micro and nano-scaled cellulose [1]. Thus, the possibilities of cellulose usage in versatile traditional and advanced materials and products widened.

One of new areas for cellulose usage is various biomedical applications – biomaterials, pharmaceuticals, medical devices. The expected requirements for such applications are very high in terms of non-toxicity, stability and biocompatibility. In other words, materials that are in contact with living tissue must remain stable without causing any cytotoxic or other side effects. Cellulose appears to have good potential to meet those requirements. Over the recent decades, large body of research has focused on finding new applications for nanocellulose due to its outstanding properties and some of them have even became commercially available (see e.g. [2]–[5]).

Nevertheless, in the development of new materials and solutions, there is potential to take advantage of nanocellulose's benefits in different aspects, for example, in biomaterials. One of good examples for nanocellulose implementation might be dentistry and dental materials. Dental adhesive materials have experienced significant progress during the past decades. However, there is still need for a material that could both bond to dental tissue well and provide quality bonding for long periods. Nanocellulose might be a beneficial component in dental adhesive composition. However, to the best of the author's knowledge, the use of nanocellulose has neither been adopted nor researched for application in dental adhesives.

This research project aims to investigate the possibility of production of a novel dental adhesive. The work focuses on developing methacrylate-based dental adhesive with improved properties by using the potential of one type of nanocellulose – cellulose nanocrystals (CNCs). This study firstly aims to find the proper raw material – a suitable form of CNCs – and, secondly, to incorporate the CNCs into model methacrylate-based polymer matrices, so that dental adhesive performance benefits. This work consists of the following steps: first, the isolation of the CNCs by three acid hydrolysis processes (sulphuric acid, phosphoric acid and hydrochloric acid); second, improvement of the compatibility between the polymer matrix and CNCs by surface modification and third, preparation of experimental nanocomposites out of CNCs and two model polymer matrices followed by the assessment of the resulting nanocomposites.

Thesis outline

The Master's thesis comprises five chapters. The background chapter provides necessary information for the thorough understanding of the addressed problem: it describes dentin bonding aspects, requirements for the ideal dental adhesive and dental adhesive composition. In the background chapter, choice of CNCs as a component for methacrylate-based dental adhesive is justified, in addition, challenges of CNCs inclusion into the polymer matrix are described. In the third chapter, materials and methods of the experimental part of this research work are described in detail, and in Chapter 4, the results of the experiments are presented and discussed. Finally, Chapter 5 presents the conclusions of this thesis and introduces the future prospects.

2. Background for the research

2.1. Dentin Bonding and the Hybrid Layer

First, the design process of a dental adhesive includes a thorough understanding of addressed problem and medical need. The chapter describes complications in dental adhesion and adhesive system.

Oral health problems can have a serious effect on the quality of life. Although teeth are created by nature to last a lifetime, lack of care and external factors can damage teeth and cause serious problems. Tooth decay by dental caries is a serious threat to oral health of the patient, and it is important to repair cavities by filling them with dental material. Another problem is the fact that although fillings should last long, nearly half of all restorations fail within ten years, and replacing them accounts for 50 - 70% of all restorations performed due to secondary caries [6]. Thus, bonding in dentistry is a key issue. Adequate adhesion is important both for satisfactory performance of restorations and for lifetime of bonding system [7], [8].

Adhesion in dentistry literally means permanently attaching dental materials to tooth tissue. Almost all fillings at some point fail because new decay often begins at the interface of a filling and the tooth, called secondary tooth decay. Adhesive restorations only remain in the optimum condition for 3 – 5 years [9]. To prolong lifetime of dental fillings is possible by improving dental adhesive bonding and preventing marginal microleakage [10], [11].

There are three components in the relevant bonded structure: the dental adhesive and two different materials bonded together by the adhesive, i.e., dental hard tissue (dentin) and restorative material (dental filling). In the following subchapters those three components are discussed in detail.

Dentin

Tooth is a complex structure made of four different tissues (Figure 1), which differ in morphology and compositions.

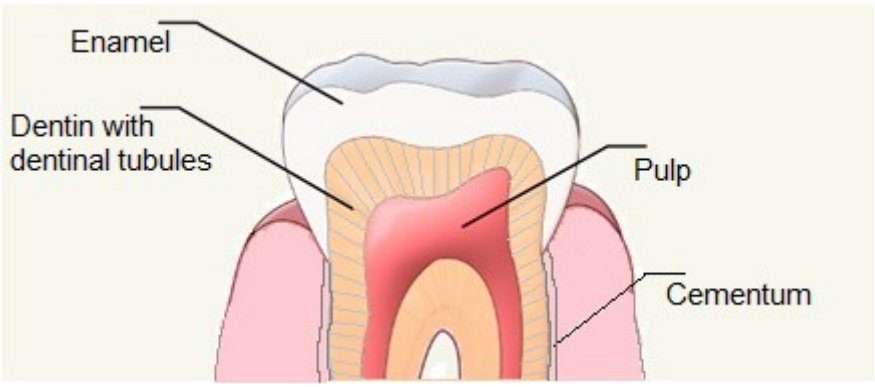

Figure 1. Schematic representation of four major dental tissues.

The hard tissue of tooth consists of outer layer and underlying dentin. Enamel is visible white-coloured protective outer layer, the hardest part of tooth, close to 100% containing hard solid structure which consists of a crystalline calcium phosphate mineral (called also hydroxyapatite and having the chemical formula ($Ca_{10}(PO_4)_6(OH)_2$). Under enamel there is dentin, it is the main tissue of tooth and makes up the majority of tooth's volume [12]. Dentin is not as hard as enamel and it is less brittle. It also supports and compensates enamel and protects the underlying living tissue – pulp.

Dentin is a heterogeneous structure, described as a vital, hydrated composite material [13]. Dentin comes in different forms, with structural components and properties that vary with location. The chemical composition of dentin consists of collagen type I (30 to 50 v/v%), water (20 v/v%) and minerals such as apatite (30 to 50 v/v%) [13], [14]. Depending on the location and condition of the dentin, the percentage ratios of components in dentin composition vary widely [12]. Structurally, dentin consists mostly of collagen fibrils and dentinal tubules. Tubules are described as tracks taken by odontoblastic cells from the dentin – enamel junction [13]. Their density and orientation vary from location to location, tubule density ranges from 10 000 to 30 000 per 1 mm^2 [15]. In terms of mechanical properties, the compressive modulus for dentin is determined between 11 and 25 GPa [16]. According to hardness tests, measuring the resistance of the dentin to deformation caused by

penetration of an indenting stylus, it varies from 30 to 70 kg/mm^2 [17]. Bending strength of the human dentine is determined between 15 and 200 MPa, and the broad range of bending strength values is a consequence of morphological and chemical variability of dentin tissue [15].

Dentin tissue is subjected to changes due to aging and diseases. Dentin tissue undergoes physiological aging process, which increases its thickness and decreases in dentin permeability [10], [11], [18]. Dental caries, an infectious microbiological disease of the teeth, causes localized dissolution and destruction of the hard tissues. Every time sugars and other fermentable carbohydrates, after being hydrolysed by salivary amylase, provide substrate for the actions of oral bacteria, weak organic acids are produced as a by-product, and those cause local pH values to fall below critical value for hydroxyapatite (~ pH 5.5). Hydroxyapatite starts to dissolve, and this phenomenon is known as demineralisation [19], [20].

Due to dentin composition, adhesion to dentin is more challenging than enamel adhesion [21]. Present organic material in composition of dentin, collagen, make the bonding also complicated. In dental adhesion, it is important to understand that dentin surface is a strong hydrophilic adherent with constant presence of dental tubular fluid coming through tubules and pressure from pulpal pressure. Organic material, collagen, makes the bonding also complicated. Smear layer is another factor affecting dentin surface properties. Achieving durable bonding to dentin is complicated, both due to the complexity of surface morphology and chemical structure, and to their variations [18].

Hybrid layer

In the formation of an adhesive bond, a transitional zone is formed at the interface between the adherent and the adhesive. Dental adhesive contacts directly with dental tissue and covers the internal surfaces of the tooth cavity by penetration into tiny nano-sized dental tubules inside the tooth. Initially a liquid material, it flows into the exposed by etching dental tubules, forming resin tags while penetrating the tissue and polymerizing in situ [22]. This resin-impregnation creates a transitional layer, that is neither resin nor tooth, but a hybrid of those two. In dentistry the

interface layer is called a hybrid layer [23]. Figure 2 provides schematic depiction of a hierarchical view of a hybrid layer and its constituents.

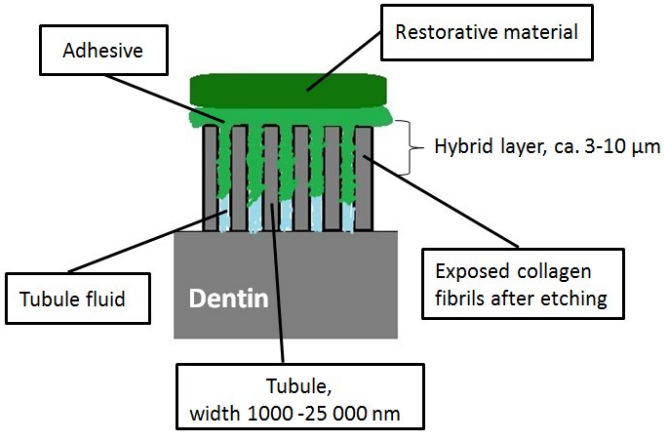

Figure 2. Schematic representation of hybrid layer.

The bonding mechanism of adhesive systems basically involves the replacement of minerals removed from the hard dental tissue by resin monomers, in such a way that the eventual polymer becomes micro-mechanically interlocked to the dental substrate [24].

Formation of the hybrid layer is critical for adhesion [10]. It is believed that the quality of the hybrid layer is a controlling factor in durability and strength and it is responsible for the transference of stress from one adherent to another [25], [26]. Resin tags, formed in the hybrid layer, contribute to the long-term stability of the bond. It is assumed that micromechanical interlocking guarantees the resistance to the adhesive debonding by two mechanisms: (i) micromechanical interaction due to polymerization *in situ* of the infiltrated adhesive monomers and (ii) chemical interaction due to ionic or covalent bonding between the functional monomers of adhesive systems and the calcium in residual dentin hydroxyapatite [22], [26]. The chemical interaction is crucial for enhancing the durability and overcoming the adhesive-interface degradation [27].

Restorative material

The material used to fill the dental cavity is called a restorative material. Dental restorative materials are high performance materials, subjected to harsh oral environment: they are subjected to a wide range of temperatures (15 – 68 °C) and pH values, together with static and fatigue loads of up to 600 N [28]. Those materials have to be able to adequately perform for long periods. Typically, in modern dentistry most dental cavity fillings are mixtures of dimethacrylate composite resins, similar to modern dental adhesives. The present composite materials in dentistry do not possess adhesive properties to bond to the tooth tissue and they exhibit hydrophobic properties, as opposed to the dentin tissue [22].

2.2. Dental adhesive

Requirements

The primary purpose of a dental adhesive is to provide a strong and durable bond between the dental surface and the restorative material [10], [18]. For good performance and accomplishing its main task, dental adhesive should fulfil the following requirements:

1. *Physical and chemical bonding.* Adhesive should create both physical and chemical bonding mechanisms with both surfaces – one hydrophilic and another hydrophobic. It means that it should be compatible with the overlaying resin composite. With dentin surface, it is a more challenging task as described previously.

2. Good wettability. The composite should have a good wetting ability in order to penetrate to the intertubular dentin. For durable adhesion to occur in the mouth, the liquid adhesive must wet the solid adherent to allow structural interaction, the stress concentration at the interface must be reduced, and the interface must be protected from degradation in the oral environment. Good adhesion between the dentin tissue and the restorative material prevents nanoleakage in the adhesive layer [10], [13].

3. Etching effect. The adhesive should provide adequate etching effect on dentin and enamel [29].

4. *Good mechanical properties.* One of the central requirements of a dental adhesive is that the mechanical properties are suitable for the task. Flexural strength

is of high importance for the adhesive in order to withstand mostly compressive forces transferred from the restorative material during service life [30].

5. *Easy, quick and safe polymerization process.* Adhesive should be cured quickly and in a simple manner by obtaining an optimal degree of conversion and good mechanical strength of the adhesive layer before the application of a restorative material [31].

6. *Hydrolytic stability.* The composite and the formed bond, having to withstand constant contact with water, should retain dimensional stability [29].

7. *User-friendliness.* As a product in service, user-friendliness is important: handling and applying the composite material should be easy for medical personnel. The application procedure of an ideal dental adhesive should be simple and straightforward, providing consistently durable and effective bonding, which is typically described in professional dental literature as “low technique sensitivity” [32]. Stability of the composite material during shelf life is important as well. All components in the composite should be biocompatible (non-toxic, not causing allergy).

8. *Remineralization function.* PO_4^{3-} ions reform damaged mineral structures of teeth. The demineralisation process, however, could be reversed by the buffering effect of hydroxyapatite dissolution products and the presence of sufficient amounts of Ca^{2+} and PO_4^{3-} in the surrounding environment. Environmental pH neutralisation above the critical level enhances precipitation of Ca^{2+} and $PO4^{3-}$ within demineralized tooth structures. This phenomenon is known as remineralization.

Dental adhesive: composition

The chemical formulations of dental adhesives vary, but in modern dentistry, a dental adhesive typically is in the form of a liquid solution, consisting of few components. The main ingredients of a dental adhesive are: resin co-monomers, initiator system, solvents, inhibitors and sometimes fillers [31], [33]. Each of the matrix components is described in detail in the following sections.

Co-monomer system

The matrix of most modern light-cured resin composite materials used consist of methacrylate-based monomers [29], [34]. In this study, two most widely used co-

monomer system are used as model resin matrices for experimental dental adhesives:

1. 2-hydroxyethyl methacrylate (HEMA) and triethylene glycol dimethactylate (TEGDMA) co-monomer solution with initiator system: Camphorquinone (CQ) and 2-(dimethylamino) ethyl methacrylate (DMAEMA);
2. Bisphenol A Glycidyl Methacrylate and TEGDMA co-monomer solution with initiator system: CQ and ethyl-4-(dimethylamino) benzoate (EDMAB).

The monomer solution HEMA/TEGDMA has a low viscosity, which is beneficial for the product application. It is also hydrophilic, which increases its compatibility with dentin, but it has relatively low mechanical strength in polymerized form. Second model co-monomer system, bisGMA/TEGDMA, is more viscous and more hydrophobic compared to the first one, but in polymerized form it possess better mechanical properties.

HEMA

In the form of a colourless liquid, HEMA is an aliphatic low molecular weight acrylic monomer, with a hydrophilic pendant group. The monomer is soluble in water, ethanol and acetone. After polymerisation, however, poly (2-hydroxyethyl methacrylate) (PHEMA) is a flexible cross-linked gel-like polymer in water, also called a hydrogel [35]. PHEMA is amphiphilic, containing both hydroxyl groups and hydrophobic groups (methyl and ethelyne groups). PHEMA has high water sorption properties, and behaves differently on the surface and in bulk, thus having tissue-like character [36].

PHEMA is widely used as a solvent and adhesion-promoting agent in dental adhesives, with relative general biocompatibility, chemical and thermal stability but having a serious drawback for its use in medical applications - allergic effect [37]. Being hydrophilic by nature, PHEMA provides good wettability of dentin [31]. Thus, it has a positive influence on the bond strength. On the other hand, the high water uptake of PHEMA leads to swelling and reduces mechanical strength. The amount of PHEMA in the adhesive has an effect on mechanical properties – the higher the amount, the lower the mechanical properties [38]. Another benefit of HEMA in dental applications is its possibility to polymerize rapidly in the presence of light. Curing by blue light (470 nm) is less harmful for a living tissue and produces lower amounts of

heat during polymerization than for example UV light, used previously in curing dental composites [34].

BisGMA

BisGMA or “Bowen-resin”, called after its inventor, is a hydrophobic monomer solution with high viscosity. Due to its high molecular weight, BisGMA provides rapid hardening and the resulting polymer is characterized by superior mechanical qualities. Due to a presence two voluminous aromatic rings in the structure, bisGMA is quite rigid monomer and has a negative effect on conversion rate, as the polymerizable methacrylate groups will have difficulty finding a matching methacrylate group [31].

TEGDMA

Co-monomer TEGDMA is among most frequently used cross-linkers in adhesive systems [31]. It carries two reactive double bonds and therefore, it is able to form covalent bonds between the polymer chains while polymerized. Cross-linking improves the mechanical properties of the composite [33]. Compared to HEMA, a small and amphiphilic methacrylate, TEGDMA has higher molecular weight and it is more hydrophobic. Overall, TEGDMA is characterized as a highly flexible, low molecular weight and low viscosity monomer. And despite its cytoxity – a quality similar to other methacrylate monomers [39] – TEGDMA is frequently used in dental composites due to its characteristics that contribute to high mobility during polymerization, consequently favouring conversion [40].
In the resin mixture bisGMA/TEGDMA, TEGDMA functions also as a diluent component. Being significantly lower in viscosity than bisGMA, TEGDMA improves the application of a dental adhesive and its penetration into dental tubules [41].

Photo-initiating system

Room-temperature photo-polymerization of a dental adhesive resins is generally initiated by photo-initiating system, consisting of initiator and co-initiator. The efficiency of a photo-initiating system affects clinically important properties for a

dental adhesive performance, such as the rate of polymerization, the depth of cure and the final monomer conversion [42].

Initiator CQ

Methacrylate monomers in dental adhesives polymerize by radical polymerization reactions in the presence of light. The photo-initiator is an important component in visible light-induced polymerization. Small amounts of photo-initiator start the reaction [43]. CQ is by far the most widely used visible-light photo-initiator in biomedical applications [44], [45], even despite its proven cytotoxicity [46]. CQ is a yellow-coloured powder, which influences on the colour of the adhesive already at small amounts. LED light-curing unit device has a narrow emission spectrum with visible blue light and it is optimal to use with CQ [31]. CQ produces free radicals on exposure to 450–500 nm radiation with a peak at 470 nm. CQ itself can photo-initiate polymerization, but at a low reaction rate and therefore, amine-containing compounds are widely used as co-initiators for CQ [47].

Co-initiator DMAEMA

The co-initiator (amine compound) plays a critical role in the photo-initiation process [48]. A co-initiator does not absorb light but interacts with the activated photo-initiator, which generates a reactive free radical and initiates polymerization [49]. Both the type of co-initiator and initiator's ratio influence the quality of the polymerization.

DMAEMA is a co-initiator, carrying a methacrylate group, and together with CQ it is the most commonly used photo-initiator system in current photo-activated dental materials [50], [51]. However, the disadvantage of DMAEMA is its low chemical stability at certain conditions, for example, it has been proved to be ineffective for acidic monomers because of its strong basicity [52].

Co-initiator EDMAB

EDMAB is a popular co-initiator in dental restorative materials due to its high efficiency [53]. However, it does have some limitations, such as sensitivity to oxygen inhibition [54], being unstable under acidic conditions and, as a result, unstable in

acidic dental resin composition [55]. Furthermore, EDMAB could be potentially cytotoxic [56].

Inhibitor

Inhibitors are added to dental adhesives to promote their shelf life. Initiator or co-initiator molecules during storage or transportation may decompose or react spontaneously, forming radicals. Inhibitors are able to trap free radicals, originating from prematurely reacted initiators. Hydroquinone (HQ), also known as benzene-1,4-diol, is a typical inhibitor, used in dental adhesives. HQ has two hydroxyl groups bonded to a benzene ring. Only minute amounts are sufficient to promote the shelf life of dental adhesives without compromising speed of polymerization [31].

Solvents

Solvents are important components of an adhesive system. Solvents are added to lower the viscosity of the formulation of the dental adhesive thus improve wettability of the surface and assure the diffusion of the liquid monomer mixture into the demineralized dentin. After the application of a liquid monomer mixture, the solvent should be eliminated, otherwise the remaining solvent may affect negatively on polymerization due to the dilution of monomers [57]. Thus, evaporation rate is an important property of a solvent for dental adhesive [58]. Typically solvent evaporation is promoted by strong blasts of air whereby the dental adhesive is further *in situ* polymerized. Water, ethanol and acetone are among the commonly used solvents [31]. In this research, solvents are not used in dental adhesive composition.

Summary of all the components, forming the polymer matrices, used in this research, is presented in Table 1. The components are ordered according to their weight percent in adhesive mixture.

Table 1. Dental adhesive components (polymer matrix) used in this study.

Component	**Molecular weight (g/mol)**	**Molecular Formula**	**Chemical structure**	**Description**
HEMA	130	$C_6H_{10}O_3$	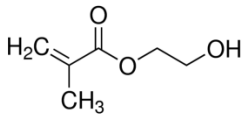	monomer
bisGMA	513	$C_{29}H_{36}O_8$	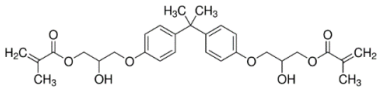	monomer
TEGDMA	286	$C_{14}H_{22}O_6$	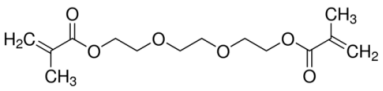	co-monomer
DMAEMA	157	$C_7H_{14}NO_2$	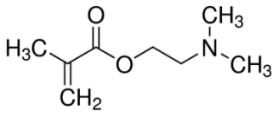	co-initiator
CQ	166	$C_{10}H_{14}O_2$	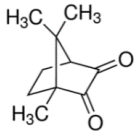	photo-initiator
EDMAB	193	$C_{13}H_{19}NO_2$	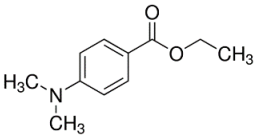	co-initiator
HQ	110	$C_6H_6O_2$	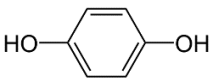	inhibitor

2.3. CNCs as a potential component for dental adhesives

2.3.1. General

Particles of different size and shape, generally called fillers, could be added to the polymer matrix to reinforce a polymer structure and improve certain properties. Modern trend is usage of nano-sized particles, in which case the resulting material is called a nanocomposite.

Traditionally, dental adhesives have not contained any fillers [8]. From the beginning of 2000s, mechanical properties were raised as an important factor in the overall bonding performance of the bonded system [30]. The most straightforward way to impact mechanical strength of a polymer material is to transform the material into a composite by adding reinforcing fillers to the matrix.

Several researchers studied the effect of nano-sized fillers addition on the mechanical properties of dental adhesives. Thus, added silanized silica nanofillers increased microtensile bond strength of adhesives [59] and hydroxyapatite nanoparticles successfully reinforced a commercially available dental adhesive [60]. Moreover, the newest generation adhesive systems have started to incorporate a reinforcement part, ranging from 0.5 wt.% to 40 wt.% [7], [59], [61].

Nanocellulose is a novel sustainable raw nanomaterial, obtained from a naturally occurring polymer – cellulose – by treating a plant-based fiber with mechanical or chemical methods. Nanocellulose is a general term for a group of nano-sized cellulosic materials, including cellulose nanofibers, bacterial nanocellulose and CNCs (see e.g. [62]–[64]).

In this study CNCs are proposed as a potential component for a dental adhesive to improve its performance, and in this subchapter the author focuses on CNCs, including their beneficial properties for dental adhesives and the possibility of inclusion of CNCs into methacrylate-based matrices described in detail previously.

CNCs are described as highly crystalline nanoparticles obtained from fibers and fibrils after the removal of the disordered cellulose domains by acid hydrolysis. There is potential in CNCs to improve dental adhesive performance due to their

characteristics, such as size, mechanical properties, relatively low density (ca. 1.5 – 1.6 cm^{-3}) and biocompatibility. Additionally, renewability, availability, inexpensiveness and reproducible quality make it an attractive raw material for dentistry.

For dental adhesives, the size of a filler is of primary importance. The preferred size for the filler is less than 20 nm [31]. CNCs have a rod-like shape with different dimensions depending on the type of production and the source material [65], [66]. For example, CNCs, prepared from cotton and cotton linters, are reported to have a diameter of 5 - 30 nm and lengths ranging from 70 to 500 nm [63].

Nanocellulose is stated to be biocompatible and a material of low toxicity [3]–[5], [67], [68]. This property is essential for dental materials, contacting directly with living tissue. Therefore, CNCs are attractive components for dental materials compared to such nanoparticles that induce cytotoxic effects.

Extensive research during the past two decades has shown that CNCs are promising reinforcing components, able to increase the strength of nanocomposite materials (see e.g. [63], [64], [69], [70]). The improvement of mechanical properties is possible already at low load: an addition of a small volume fraction of nanocellulose results in a nanocomposite material with a significantly stronger mechanical performance than that of an unreinforced matrix [71], [72]. CNCs are promising for the reinforcement of both synthetic [73] and natural polymer matrices at low loading levels [74], [75]. CNC has high tensile properties, with theoretically estimated Young's modulus at around 150 GPa and tensile strength up to 10 GPa [76], [77]. Few studies have shown the potential of nanocellulose in dental applications as a reinforcement agent. Works by Silva et al. [78], [79] showed that incorporation of CNCs prepared by sulphuric acid hydrolysis from eucalyptus in commercial dental glass ionomer cement improved the mechanical strength. The addition of even a small amount of CNCs (less than 1 wt.%) in the GIC led to significant improvements in all of the mechanical properties evaluated: both compressive strength and elastic modulus increased. Thus, CNC is a potential reinforcement component for a dental adhesive, able to improve the mechanical properties without significantly increasing viscosity of the resulting nanocomposite,

due to CNCs proven ability to reinforce nanocomposites at small CNCs load and its relatively low density.

2.3.2. CNCs preparation

CNCs are mainly isolated by acid hydrolysis from pure cellulosic material under controlled conditions such as temperature and time [63]. Several acids can be used for CNC production and the acid of choice affects the characteristics of the resulting CNCs. Thus, sulphuric acid, the most commonly used for CNC isolation, produces CNCs with charged sulfate groups (SCNCs), that promote dispersion of the CNCs in polar solvents [70]. Hydrochloric acid has also been used in CNC production [63]. A recently reported method of CNC preparation by HCl vapour is simple with yields of around 97%, and the resulting product is in macroscopic form, convenient for handling and further modification [80]. Because CNCs prepared by HCl hydrolysis (HCNC) do not have negative charge, they do not form dispersions tending to precipitate, and have limited ability to disperse in aqueous suspensions [70]. Another acid used for CNC preparation is phosphoric acid (PCNCs). PCNCs have anionic phosphate half-ester groups that facilitate the dispersion of CNCs in water, but due to generally lower charge, they are less stable than SCNC dispersions [81], [82]. There is very limited literature about preparation of CNCs by phosphoric acid hydrolysis, although PCNCs might be potentially attractive as reinforcement in nanocomposite used in dentistry due to the presence of phosphate groups, often more compatible with living organisms. In dental hard tissues a demineralization process occurs due to dental caries and aging. It is reversible in the presence of sufficient amounts of calcium and phosphate ions (Ca^{2+} and PO_4^{3-}) in the surrounding environment, as a process known as remineralization. Thus, phosphate ions might contribute to remineralization of tooth tissues [83]. In this research work three types of CNCs - HCNC, SCNC and PCNC were prepared as starting materials, and the use of each type as a reinforcement part in the nanocomposite was evaluated.

2.3.3. CNCs modification and inclusion in a composite matrix

Inclusion of any of the above described CNCs (HCNC, SCNC, PCNC) in a polymer matrix is challenging due to the nature of cellulose material which is polar and hygroscopic whereas the polymer matrix is often more hydrophobic. However,

compatibility between CNCs and a co-monomer solution, resulting in their uniform dispersion in a host polymer matrix, is a critical factor, affecting the physical properties and mechanical performance of a resulting nanocomposite [62], [69], [70], [77]. By changing CNCs surface chemistry, it is possible to achieve good dispersibility of CNC in the co-monomer solution before the polymerization.

Chemical functionalization of CNCs happens through the reaction of abundant hydroxyl groups present on the surface. The main challenge in modification is the choice of the proper chemical reagent and medium without undesirable bulk changes, such as aggregation or a loss in CNCs mechanical properties [63], [84]. The functionalization of CNC surface is possible through covalent chemical modification and includes esterification, etherification, oxidation, silylation and polymer grafting reactions [63]. Many of those modification methods are challenging, because CNCs hydroxyl groups are generally less reactive than other corresponding alcohols, due to poor dispersion in organic solvents and laborious purification process [70]. An alternative to chemical surface modification is the adsorption of surfactants or polymers on CNC surface, which reduces surface energy and can improve colloidal stability in the solvent [63].

In this work for better compatibility and obtaining good dispersibility of CNCs in the polymer matrices it was decided to introduce vinyl functional groups on CNC surface through a silylation reaction. Silanes are employed as coupling agents to improve the adhesion between interfaces in different adhesives. Silane compounds, called also quite often in literature silane coupling agents, are synthetic organic-inorganic chemicals usually used for bonding dissimilar materials, also widely used in dentistry to bond resins to silica-coated metals, ceramics and resin composites. They are also important in new dental composite development. [85], [86]. Silanes have bifunctional groups, which allow them to bind to different phases by creating bridges in between them. Silanes, having different organofunctionalities, typically amino, mercapto, glycidoxy, vinyl, or methacryloxy groups, might interact with the polymer matrices depending on their reactivity or compatibility towards the polymer. [85], [87].

It has been demonstrated that the alkoxysilanes react with the hydroxyl groups of cellulose. Activation of alkoxy groups is necessary in the reaction with cellulose, in which more reactive silanol groups towards cellulose are formed [88]. There are

examples of successful introduction of different functional groups on the CNC surface through silylation and thus improvement of compatibility between polymers and cellulosic material. A group of researchers [89] has shown that modification of CNCs with a silane compound bearing an amine end group contributes to the improvement of filler-matrix adhesion. Incorporation of silylated CNCs from mengkuang leaves into poly(vinyl chloride) increased the tensile strength of the composite. Another research showed that SCNCs obtained from tunicin were successfully modified with silane compounds (alkylchlorosilanes), keeping the core almost intact, and further formed good dispersions in organic solvents of medium polarity [90].

In the present study, 3-methoxysilyl propyl methacrylate (MPS) was used for CNC surface modification due to several reasons. MPS is a commercially available silane compound with a functional group similar to that of the matrices used in this work. MPS has a short hydrocarbon chain, with functional methacrylate group and methoxy (–O–CH_3) group on the other end, which can adhere to the CNC surface and a methacrylate group that can polymerize with the monomer. Thus, introducing chemical bonds between the polymer and the CNC in the nanocomposite material, loads are transferred between the two phases and in this way, the strength of the composite improves. Modification of CNCs by attaching vinyl groups might benefit by possible simultaneous covalent bonding and formation of highly cross-linked network with the polymer. After initiation, the polymerization reaction occurs across the vinyl double bonds of the methacrylate groups and as the reaction progresses, the double bonds of the methacrylate groups of HEMA / TEGDMA can react also with the vinyl groups of the modified CNCs. The expected polymerization reaction in the presence of modified CNCs is presented in Figure 3.

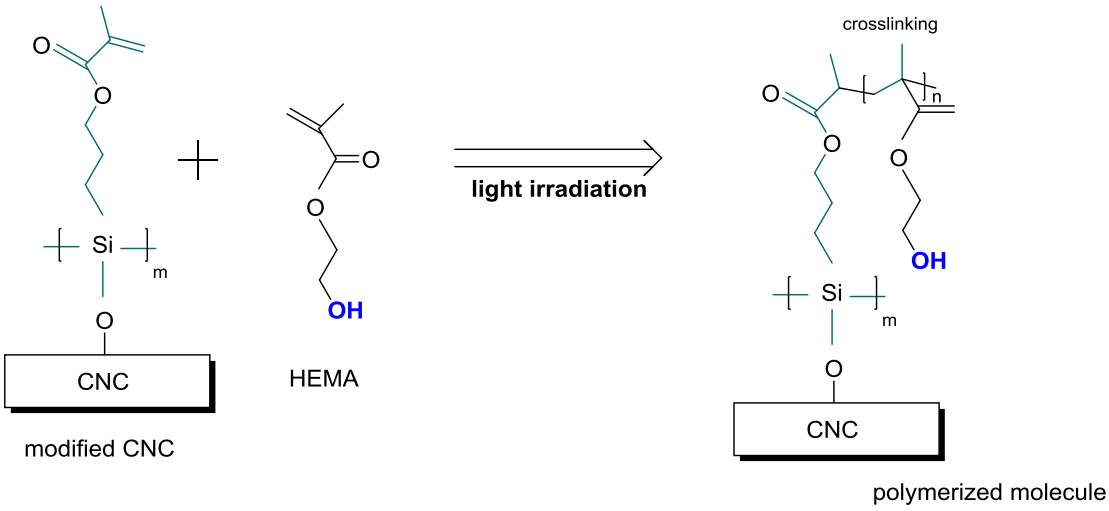

Figure 3. Simplified schematic representation of the expected copolymerization of HEMA and CNCs (CNCs are depicted as rectangular).

It was important also that the reaction proceeded under reasonable conditions, and without compromising safety. It should be mentioned as well that MPS is a typical silane compound used in dentistry [86]. For example, MPS was used to modify glass fiber filler particles, thus yielding a better dispersion and wetting for filler particles in a polymer matrix [85]. Surface silanization with MPS on cellulosic fibers typically is carried out through the condensation reaction between hydroxyl groups on the cellulose surface and further curing to form chemical bonds. The recently published study by Beaumont *et al.* [91], on the other hand, introduces a well-developed protocol of silylation for nanocellulose materials avoiding solvent-exchanging steps and thermal treatments.

HCNCs modification by vapour deposition

The dispersion of CNCs — throughout the reaction and purification processes – is a bottleneck in CNC modification. Therefore, chemical vapour deposition (CVD) was attempted as a convenient and neat pathway of modification for HCNCs in this study. CVD was used to deposit films on the surfaces and efficiently applied for nanocellulose [92], [93]. It was proposed that as a silane compound, MPS under certain conditions becomes volatile and creates a deposit on the cellulose surface, reacting further with the abundant hydroxyl groups of HCNCs.

Modification of PCNC and SCNC in aqueous media

For SCNCs and PCNCs in the form of freeze-dried particles, silylation in aqueous media has been suggested. In this study, CNCs were modified in similar way to the work of Abdelmouleh *et al.* [88], proving that silane coupling agents display a good affinity toward cellulose at certain conditions. Prehydrolyzed in ethanol/water, a silane compound with silanol groups instead of methoxy groups, was first physically adsorbed onto the CNC surface through hydrogen bonds, finally the long chain hydrocarbon was covalently linked to the surface of CNC through Si-O-C bonds which formed via the condensation reaction between hydroxyl and silanol.

During the work under this project the new aqueous silanization protocol for nanocellulosic materials was published [91]. Introduction of the functionalized group (vinyl group) in this approach was made avoiding thermal treatment and thereby avoiding the irreversible changes in CNCs such as hornification and agglomeration of nanocellulose. So on the latest stages of the research work, this new simple modification pathway was implemented.

3. Experimental part

The objective of the experimental work is to produce dental adhesive with CNC-reinforced nanocomposite used as dental adhesive with improved properties. In order to achieve the main research objective, this work is divided into three specific aims:

1. Choice of a suitable type of CNC.
2. Homogenous dispersion of CNCs in the polymer matrices.
3. Preparation of experimental nanocomposites with CNCs and evaluation of their mechanical properties, degree of monomer conversion and morphology.

General scheme, representing the experimental plan with the main stages, is shown in Figure 4.

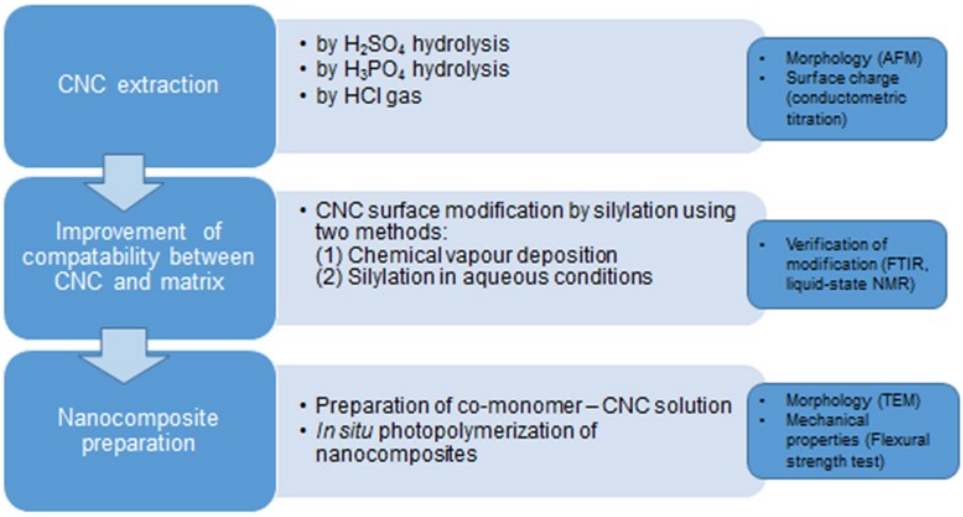

Figure 4. Experimental plan.

3.1. Materials

Chemicals

CNCs were prepared starting from Whatman 1 filter paper (Whatman GmbH, Dassel, Germany). Deionized water (Milli-Q, Millipore corporation, resistivity 18.2 MΩ×cm) was used in all experiments. All other chemicals used in the work are summarized in Table 2. The chemicals were applied as purchased without further purification.

Table 2. Chemicals used in the work and suppliers.

Chemical	Purity, %	CAS number	Manufacturer
(1R)-(−)-Camphorquinone, (CQ)	> 98.5	10334-26-6	Sigma-Aldrich Finland Oy
2-(Dimethylamino)ethyl acrylate, (DMAEMA)	> 97.5	2439-35-2	Sigma-Aldrich Finland Oy
2-hydroxyethyl methacrylate, (HEMA)	> 96.5	868-77-9	Sigma-Aldrich Finland Oy
3-Trimethoxysilyl propyl methacrylate, (MPS)	> 98.0	2530-85-0	Sigma-Aldrich Finland Oy
acetone, 100%	≥ 99.6	67-64-1	VWR Chemicals
Bisphenol A Glycidyl Methacrylate, (bisGMA)	> 85	1565-94-2	Esschem Europe
ethanol, Aa grade	> 99.5	64-17-5	Altia oyj Finland
ethyl-4-(dimethylamino) benzoate (EDMAB)	≥ 99%	10287-53-3	Sigma Aldrich Finland Oy
hydrochloric acid, 99,8%	≥ 99.8	7647-01-0	AGA, Sweden
phosphoric acid	> 85.0	7664-38-2	Analar VWR
sulphuric acid	> 95	7664-93-9	Emsure Germany
triethylene glycol dimethactylate, (TEGDMA)	> 95	109-16-0	Sigma-Aldrich Finland Oy

3.2. CNC preparation and modification

Sulphuric acid hydrolysis

SCNCs were prepared as described elsewhere [94] with slight modifications. Grinded 15 g of Whatman 1 filter paper was hydrolyzed with sulphuric acid (175 ml, 64 wt.%) at 45°C for 45 minutes. After the hydrolysis, the mixture was diluted with 3 l of water. Then, SCNCs were isolated and purified by centrifugation and dialysis against water (membrane: SpectraPor® 7, MWCO 6kDa) to a conductivity of < 5µS, respectively. After the first dialysis cycle, the counter ion of sulphuric acid half-ester groups was exchanged (-SO_3H to SO_3Na) by adjusting pH to 7 with 0.1 M NaOH solution, followed by freeze-drying using a Labconco lyophilizer for 3 days. Finally, SCNCs were purified by Soxhlet extraction with ethanol for 48 hours in order to remove surface impurities.

Phosphoric acid hydrolysis

PCNCs were prepared according to previously reported conditions [81] with slight modifications. The batches PCNC 23418 and PCNC 13818 were prepared as follows: 2 g of Whatman 1 filter paper was soaked in 100 ml of water for 15 minutes and then ground with a regular kitchen blender to obtain a pulp-like mixture. The mixture was cooled down for 15 minutes on ice bath and then mixed with phosphoric acid until a final acid concentration reached 10.7 mol/l. The reaction vessel with the mixture was placed in an oil bath and kept at 100° C at constant stirring for 90 minutes. The resulting reaction mixture was cooled to room temperature, and PCNCs were isolated and washed with water by repeated centrifugation steps (centrifuged at 11000 rpm, 15 minutes) until a pH of ≥ 2 was reached, followed by dialysis against (membrane: SpectraPor® 7, MWCO 6 kDa) water to pH 7. centrifuged at 11000 rpm for 15 minutes to separate the acid and PCNCs. PCNCs were washed with water and were centrifuged again (11 000 rpm, 15 minutes). This procedure was repeated several times, until the pH reached ≥ 2. The mixture was dialyzed against water, until the pH of surrounding dialysis tubes was ca. 7. The final PCNCs dispersion was sonicated for 15 min using a tip sonicator on an ice bath. The dispersion was then frozen in liquid nitrogen, and lyophilized for 3 days.

In the following study, the hydrolysis process was optimized, and the batch 251018 was prepared according to the optimized procedure. 267.5 ml of 14.6 M phosphoric acid was diluted to 10.7 M by adding water. 2 g of Whatman 1 filter paper were ground by a typical coffee grinder and mixed with 10.7 M phosphoric acid. The reaction vessel with the mixture was placed in an oil bath, covered with foil and heated under reflux at 100 °C at constant stirring for 90 minutes. The resulting reaction mixture was purified and then freeze-dried as described previously.

Hydrochloric acid vapour hydrolysis

Whatman 1 filter paper was hydrolyzed with HCl acid vapour as reported [80] in a custom-built reactor, washed with water (2 × 15 min, 300 ml) and dried overnight in a fume hood.

Dispersion behaviour of SCNC, HCNC and PCNC

For evaluation of dispersion behaviour of the prepared CNCs and estimation the suitable concentration of CNCs in further preparations of the nanocomposites, freeze-dried SCNCs and PCNCs at different weight concentrations up to 15 wt.% (1, 3, 5, 7, 10 and 15 wt.%) were dispersed in prepared co-monomer solution HEMA/TEGDMA (80/20 w/w%). For this purpose of CNCs (HCNC, SCNC, PCNC) were weighed to a glass tube and mixed with the prepared solution of HEMA/TEGDMA (80/20, v/v). Freeze-dried SCNCs, and PCNCs were dispersed as they were prepared, however, HCNCs, as obtained from hydrolysis with gaseous HCl, in a form of a solid paper sheet, were gently crushed and then mixed with HEMA/ TEGDMA solution. Resulting suspensions were observed immediately after mixing and after an hour.

Modification of CNCs surfaces by silylation

The silylation modification was performed for each type of produced CNCs. For all the modifications same silane compound (MPS) was used. For each type of CNCs appropriate reaction protocol for modification was chosen. Thus, for the HCNCs in a macroscopic form, it was possible to perform the modification through CVD, while

for the freeze-dried SCNCs and PCNCs, the modification was performed in liquid media.

Modification through CVD

Silylation of HCNCs was carried out in a desiccator, following a method adapted from reference [93] with modifications. Approximately 5 ml of MPS was poured onto the bottom of the desiccator. HCNCs (approximately 0.5 g) were placed onto the desiccator grid, approximately 2 cm above the liquid reagent (MPS). The desiccator with an opened valve was placed into a vacuum oven with controlled nitrogen flow, which was vacuum-pumped from the outlet as shown in Figure 5.

Figure 5. The CVD reactor in the vacuum oven with HCNCs placed on the grid.

With the open valve of the desiccator at equilibrium atmosphere of concentrated MPS vapour was allowed to evaporate freely and absorb on HCNCs surface. The pressure was set to 100 mbar and a continuous slow nitrogen stream was provided to eliminate the hydrogen chloride formed. The time and the temperature conditions varied in the different runs: 1). Temperature 60° C, reaction time: 1 h, 8 h and 24 h and 2). Reaction temperature 80° C, reaction time: 1 h, 4 h. The modified samples were named as mHCNC_60/1, mHCNC_60/8, mHCNC_60/24, mHCNC_80/1 and mHCNC_80/4. After modification, the samples were purified by Soxhlet extraction with ethanol for 15 hours to remove byproducts.

Modification in aqueous media (SCNCs and PCNCs)

Method 1

Modification of SCNCs and PCNCs was performed similarly to that in the work [88] with changes. First, MPS (3.1 ml, 200 mmol/l) was pre-hydrolyzed in an ethanol/water mixture (80/20 v/v) for 2 hours at room temperature. Freeze-dried SCNC or PCNC were dispersed in ethanol/water (80/20 v/v) and sonicated for 6 minutes in an ice bath. Secondly, the reaction mixture with pre-hydrolyzed MPS and 1 wt.% SCNCs or PCNCs in the total reaction mixture was stirred at room temperature for 2 hours. After the reaction was completed, the reaction mixture was precipitated by a few drops of acetone and poured into a foil dish, and left to sediment overnight. The next day, the residue was thermally treated at 110°C in a vacuum oven for 2 hours, and further purified by Soxhlet extraction with ethanol for 15 hours. Modified SCNCs (called in the work mSCNC1) or PCNCS (called in the work mPCNC1) were dispersed in water and freeze-dried for the further application.

Method 2

SCNCs and PCNCs were modified according to the new silanization protocol [91] with changes (named in this study as Method 2). Freeze-dried PCNCs or SCNCs (1 g) were dispersed in 100 ml of water and sonicated for 5 minutes on ice bath using a tip sonicator. To 1 wt.% PCNCs suspension in water, 1 ml of 0.5 M HCl was added, followed by adding 1.1 g of MPS (4 mmol). The solution was stirred at room temperature for 30 minutes. After addition 2 ml of 0.5 M NaOH, the reaction mixture was stirred at room temperature for 2.5 hours. After the reaction was completed, the mixture was immediately centrifuged at 11 000 rpm for 15 minutes in Eppendorf Centrifuge 5804 R, and the supernatant was removed. CNCs were washed in turns with water, acetone and water (100 mL water, 50 ml acetone and 2 times with 100 mL water) and centrifuged (11 000 rpm, 15 minutes) after each washing step. Purified modified SCNCs (called in the work mSCNC2) and PCNCs (called in the work mPCNC2) were freeze-dried as previously described for further application.

3.3. Nanocomposite preparation

The model resin mixture HEMA/TEGDMA was prepared as follows: HEMA and TEGDMA were well mixed with Vortex mixer (with weight ratio 80/20), and to the nanocomposite, CQ (0.7 wt.%) and DMAEMA (1.05 wt.%) were added. The glass bottle with resin mixture was wrapped in aluminum foil to prevent the visible light-activated mixture from premature polymerization. Then, the necessary amount of CNC was weighed and 1 g of ready resin mixture was added to a small glass bottle. The nanocomposite was mixed using Vortex mixer for 30 seconds with additional mixing by magnetic stirrer for 15 minutes. Table 3 presents the composition of HEMA/TEGDMA-based resin.

Table 3. Composition of HEMA/TEGDMA resin.

Component	batch [g]	[wt.%]
HEMA	16.0	80.0
TEGDMA	4.0	20.0
CQ	0.14	0.7
DMAEMA	0.21	1.05
HQ	0.003	0.015
Total	20.0	100

The second model resin, containing bisGMA and TEGDMA (with weight ratio 70/30 v/v), was prepared with CQ and EDMAB as an initiator system in a similar way to HEMA/TEGDMA resin. To both model resins, the inhibitor HQ was added to prevent premature polymerization. BisGMA/TEGDMA resin was mixed with CNCs by Hauschild speedmixer at 2500 rpm for 30 seconds. Table 4 presents the composition of HEMA/TEGDMA-based resin.

Table 4. Composition of bisGMA/TEGDMA resin.

Component	batch [g]	[wt.%]
BisGMA	35	70
TEGDMA	15	30
CQ	0.30	1
EDMAB	0.30	1
HQ	0.01	0.01
Total	50.0	100

3.4. Analytical characterization

3.4.1. Characterization of prepared PCNCS

In this work, only PCNCs were subjected to characterization.

Morphology and particle size of CNCs

The morphology and the particle size of prepared PCNCs were determined by AFM. The imaging was performed with AFM MultiMode 8 scanning probe microscope from Bruker AXS INC. (Madison, WI, USA) with a J scanner in intermitted contact mode in air. Samples for AFM imaging were prepared according to reference [95]: diluted concentrations (100 mg/L) of PCNC solutions were spin-coated on silicon wafers that had previously been coated by aqueous 0.1 M solution of titanium (IV) bis(ammonium lactato)dihydroxide (TiO_2-coated wafers), followed by calcination at 600°C in oven. The AFM images were flattened in NanoScope Analysis 1.5 and further used for the particle size determination. No additional image processing was made.

Charge density of CNCs

The charge density of PCNCs was measured by conductometric titration. First, the charged groups were converted to un-ionized form by addition of HCl till pH < 3, followed by NaOH titration. Conductometic titration of CNCs was conducted as described elsewhere [96] with slight changes. PCNCs dispersion for titration was

prepared as follows: 0.2 g of freeze-dried PCNC was dispersed in 300 ml of degassed water and 1 ml of 0.5 M NaCl solution was added. 0.1 M HCl was added dropwise until pH 3 was reached (approximately 1.8 ml), degassed water was added so that the total volume of the mixture was 500 ml and afterward the mixture was stirred at least for 2 hours. The dispersion was subsequently titrated with 0.1 M NaOH-solution at rate 0.02 ml/min using a 751 GPD Titrino Metrohm (Herisa, Switzerland). In order to increase the accuracy of results, the blank solution (without PCNCs) was titrated with 0.1 M NaOH at rate 0.02 ml/min. The concentration of phosphate groups was calculated from the conductivity curves using Origin 2018 software (OriginLab Corporation, USA). The obtained titration curve consisted of three regions: 1). the slightly decreasing conductivity of the mixture due to excess of free H^+ neutralized by NaOH; 2). plateau region, in which the volume of added titrant is increased due to a consumption for weak acid titration, while the conductivity remains unchanged; 3). strongly increasing conductivity region, where the addition of NaOH resulted in an increase in conductivity due to the excess OH^- ions. The resulting values were corrected by blank titration.

3.4.2. Characterization of modified CNCs

Photoacoustic Infrared Spectroscopy

IR gives quantitative and, particularly, qualitative information on specific functional groups present in the chemical compound based on the absorption by molecules of specific frequencies in the infrared region of the electromagnetic spectrum. To investigate the chemical changes in modified cellulose nanocrystals, IR spectrum of modified and pristine nanocrystals were compared.

For determination of presence silane compound and an indication of the modification, PAS IR spectroscopy was used. Measurements were performed on RioRad FTS 6000 Spetrometer (Bio-Rad, Hercules, California, USA) equipped with MTEC Photoacoustic Model 300 (Ames, Iowa, USA) PAS-chamber. The spectra of each sample were recorded with a 4 cm^{-1} spectral resolution between 4000 cm^{-1} and 400 cm^{-1}. Prior to each set of measurements, a background spectrum was collected using a standard carbon black. The freeze-dried samples were purged by helium gas for 5 minutes prior to each measurement. The spectra were recorded and processed using Digilab WinIR Pro 3.4.1.018 software. The spectrum were collected at the range 400 scans per spectrum. For each sample three measurements were

done and the average was baseline corrected at 4000, 2000 and 468 cm^{-1} and normalized to 1424 cm^{-1}. A control reference sample with pristine CNCs was compared to the modified CNC sample.

Liquid-state NMR Analysis

Liquid-state NMR spectroscopy was used to quantitatively analyse PCNCs modification and to determine phosphate groups in the PCNCs. Both mPCNC1 and mPCNC2, and pristine PCNCs as a reference, were dissolved in the tetrabutylphosphonium acetate ([P4444][OAc]):perdeuterated dimethylsulphoxide (DMSO-d6) ionic liquid electrolyte, according to the method developed by King et al. 2018 [97]. 1H, 13C, 31P, diffusion-edited 1H, multiplicity and diffusion-edited HSQC (heteronuclear single quantum coherence) spectroscopy and TOCSY (Total Correlated Spectroscopy) experiments were measured at 65° C for the PCNCs, mPCNC1 and mPCNC2. Additionally, mPCNC1 and pPCNC2 were extracted with DMSO-d6 and methanol-d4 (CD3OD) at 65° C for 30 min. 1H experiments were then run at 27° C as a secondary method to compare how much of the siloxanes were chemisorbed, using each method. All NMR experiments were recorded using a Bruker Avance Neo and Smart Probe. Diffusion-editing was applied in the electrolyte solutions to filter out the low molecular weight species, i.e. [P4444][OAc] and non-chemisorbed siloxanes.

3.4.3. Nanocomposite characterization

Degree of monomer conversion

The degree of monomer conversion is a fundamental characteristic that affects the performance of resin based restorative materials [98], [99].The nanocomposite conversion rate was measured by Fourier transform infrared (FTIR) analysis with an attenuated total reflection module (Bruker Alpha FR-IR spectrometer, equipped with Platinum-ATR, Bruker, single reflection diamond crystal diamond crystal), as described previously [100] by detecting the C=C stretching vibrations directly before and after curing of materials. The samples (drop of liquid nanocomposite) were placed in the on the ATR crystal of a FTIR spectrometer and were simultaneously exposed to a LED irradiation and an IR analyzing light beam. Real-time IR spectra were recorded continuously for 900 seconds after the start of the photo-

polymerization. OPUS software was used to analyze and record the obtained spectra. The degree of conversion for each sample was determined from the ratio of absorbance intensities of aliphatic (C=C) band at 1648 – 1618 cm^{-1} peak and reference acrylic signal, originating from the monomer vinyl group, (C=C) band at 1618 cm-1 to 1590 cm-1 before and after light irradiation. It was calculated using the following formula:

$$Degree\ of\ conversion, \% = \left(1 - \frac{P_{aliphatic} / P_{acrylic}}{U_{aliphatic} / U_{acrylic}} \right) * 100\ \%$$

where $P_{aliphatic}$ is the absorption peak of the polymerized specimen, $P_{acrylic}$ is the absorption peak of the polymerized specimen, $U_{aliphatic}$ is the absorption peak of the monomer and $U_{acrylic}$ is the absorption peak of the monomer.

Mechanical Properties

Dentin tissue absorbs forces applied on a tooth during mastication. Thus, force resistance is a crucial property for a material, replacing dentin tissue [16]. According to the International organisation of standardization ISO 4049:2009 (E) [101] recommendations, strength of dental restorative resin composites should be evaluated using Flexural strength test [102]. Thus, by analogy with the restorative resins, the test was performed for the prepared specimen to assess the flexural strength of the prepared nanocomposites with incorporated PCNCs and modified PCNCs.

Prior to specimen preparation for flexural strength testing, the nanocomposites were stirred by magnetic stirrer for 15 minutes. Edges of a metal mould were lubricated with a mixture of wax and hexane to prevent sticking of a specimen to the mold. Using automatic pipette the mold was filled with liquid sample and polymerized using a light emitting diode (LED, wavelength: 460-480 nm, power output: 1000 mW/cm^2) for 40 seconds on one side and 10 seconds on the other. The distance between the emitting diode and the specimen was around 1 cm. The process of preparation and the necessary equipment are presented in Figure 6.

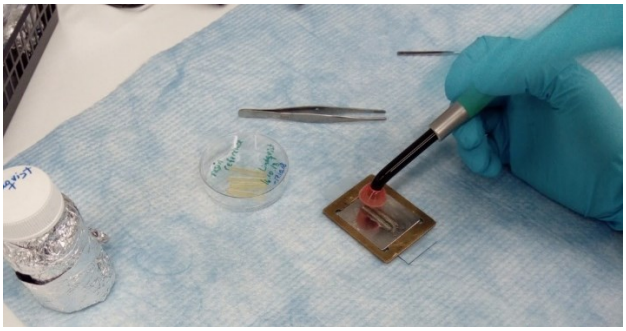

Figure 6. Preparation of specimen for Flexural strength test: rectangular mold, LED and Petri dish with specimen.

Each side of a specimen was irradiated consequently, section by section, moving the diode so that the previous section is overlapped by half. After irradiation, the specimen was removed from the mold; excess material was removed to get smooth edges and then the specimen was stored at room temperature in a petri dish prior to testing. Three different experimental groups were obtained for HEMA/TEGDMA-based nanocomposites: 1). PCNC 1 wt.%, PCNC 3 wt.%, PCNC 5 wt.%, PCNC 7 wt.%; 2). mPCNC2 1 wt.%, mPCNC2 3 wt.%, mPCNC2 5 wt.% and 3). A resin specimen without PCNCs was prepared as a reference sample. For bisGMA/TEGDMA three experimental groups were manufactured: 1). PCNC 1 wt.%, PCNC 3 wt.%; 2). mPCNC2 1 wt.%, mPCNC2 3 wt.%, and 3). a reference sample. A total of 6 bar-shape specimens were prepared with the dimension of 25 mm × 2 mm × 2 mm for each type of dental adhesive.

A universal testing machine (Lloyd LRX plus, Lloyd Instruments Ltd.), connected to a control computer from which the graphical results were obtained, was used to perform the tests as shown in Figure 7.

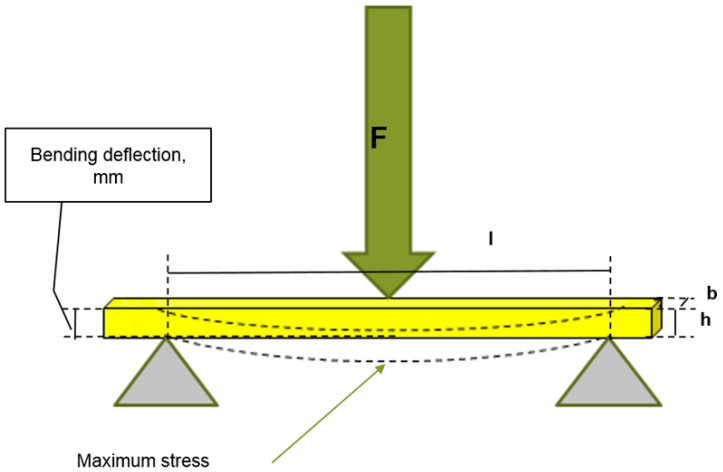

Figure 7. Flexural strength test: the bar-shaped specimen under load placed on two supports.

The bar-shaped specimen bends under applied loading at a cross-head speed of 0.75 mm/min until the specimen either reaches the yield point or fractures. Maximum loads at failure were recorded and converted to MPa by dividing the failure load by the bonded specimen surface area. The flexural strength, σ in mPa was calculated by:

$$\sigma = \frac{3 \times F \times l}{2 \times b \times h^2}$$

where F is the maximum load applied on the specimen (N), l is the distance between the supports (mm), b is the width at the center of the specimen measured immediately prior to testing (mm) and h is the height at the center of the specimen measured immediately prior to testing (mm). Means and standard deviations were obtained for each sample group.

Structural analysis of the nanocomposites by light microscopy

Preliminary study of the morphology of the experimental nanocomposites was performed by Leica DM2500 microscope (Leica Microsystems CMS GmbH) equipped with Leica EC3 camera. The unpolymerized nanocomposites in liquid state were examined by light microscopy.

TEM study of the nanocomposites

For imaging and evaluation of CNCs distribution in the polymer matrix, Transmission Electron Microscopy (TEM) was used. Polymerized by light irradiation specimen was microtomed into thin sections by ultramicrotome (Leica EMFC7). First, a Diatome Cryotrim 45 knife was used for regular trimming at room temperature to create a pyramid-shaped sample (Figure 8a) with sides inclined at an angle of 45˚. The sample was then sectioned into 100 nm thin specimen using Diatome Ultrasonic 35. The specimen was floated on water and placed on a 200-mesh copper grid with lacey carbon support film. The image in Figure 8b presents the magnified specimen placed on a carbon-coated grid. The specimen was allowed to dry at ambient temperature for 48 h prior to imaging.

a)

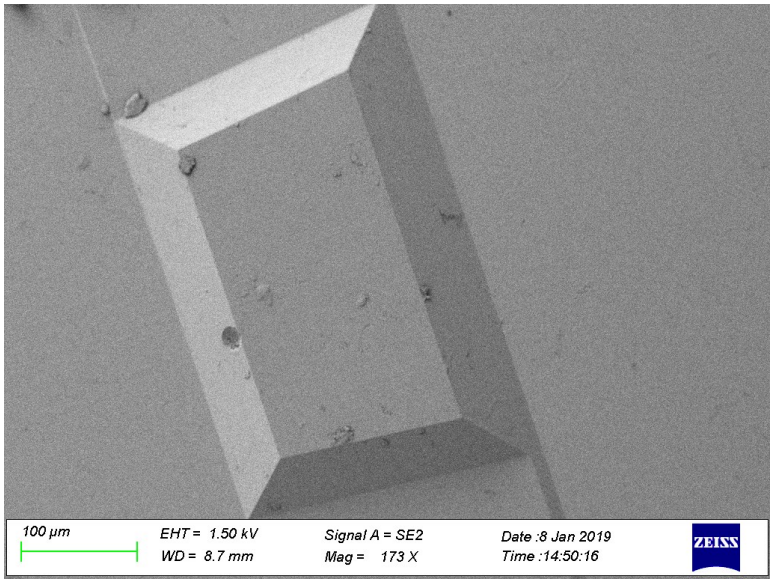

b)

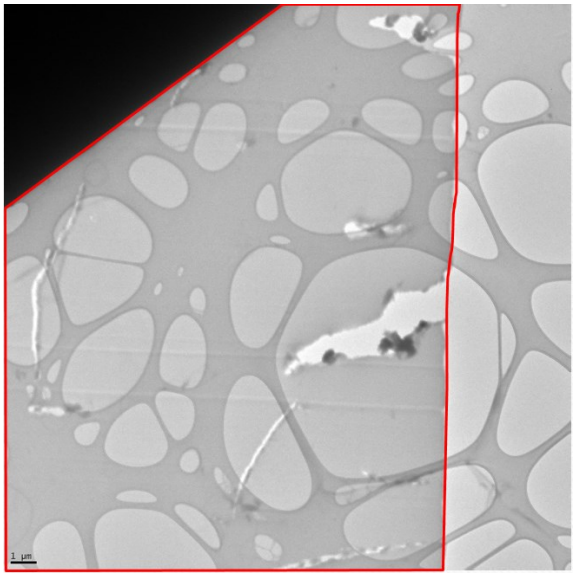

Figure 8. Sample preparation for TEM imaging: a) trapezoid-shaped cut specimen and b) TEM image of the polymerized nanocomposite specimen on the supportive carbon-coated grid, the specimen is circled in red.

TEM images were collected using JEM 3200FSC field emission microscope (JEOL) operated at 300 kV in bright field mode with Omega-type Zero-loss energy filter. The images were acquired with Gatan Digital Micrograph® software while the specimen temperature was maintained at -187° C.

4. Results and discussion

4.1. Characterization of prepared PCNCS

Three batches of PCNCs (batch 23418, batch 13818 and batch 251018) were prepared by phosphoric acid hydrolysis following the procedure described in Camarero Espinosa *et al.*, [81] at same reaction conditions (hydrolysis at 100° C for 90 minutes, 10.7 M phosphoric acid concentration). It was noticed, that the reaction mixtures of three PCNCs batches varied in colour at the end of hydrolysis from light brownish to almost white, as can be seen in Figure 9. Only the reaction mixture of batch 251018, prepared at more controlled conditions had slightly yellowish colour as it was reported in reference [81]. Typically, the colour of PCNCs reaction mixture changes during hydrolysis process from white to yellowish, thus indicating the degradation of amorphous regions of cellulose and completion of hydrolysis process. However, the observed white colour of reaction mixture might point to incomplete hydrolysis, while the brownish colour of reaction mixture might indicate degradation of crystalline regions. Also presence of impurities in the reaction mixture might contribute to darker colour of the mixture.

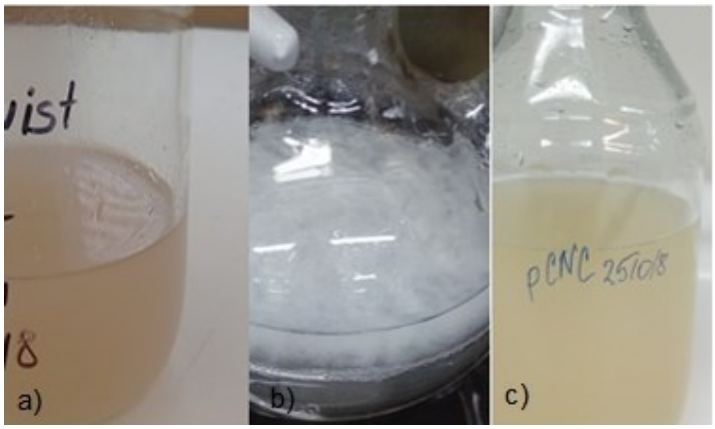

Figure 9. Reaction mixture: a) PCNC batch 23418, b) PCNC batch 13818 and c) PCNC batch 251018

Resulting freeze-dried PCNCs from different batches varied too: powder-like freeze-dried PCNCs (batch 23418) differed from aerogel-like PCNCs (batch 251018) (Figure 10).

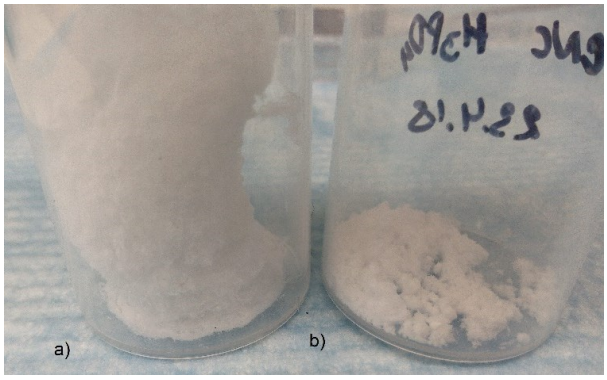

Figure 10. Freeze-dried PCNCs: a) air-gel like PCNCs (batch 251018) and b) powder-like PCNCs (batch 23418).

The concentration of phosphate groups for the PCNCs was determined by conductometric titration and was found to be 55 mmol/kg for batch PCNC 23418, 80 mmol/kg for the batch PCNC 13818 and 72 mmol/kg for batch PCNC 251018. The curves obtained by titration can be seen in Figure 11.

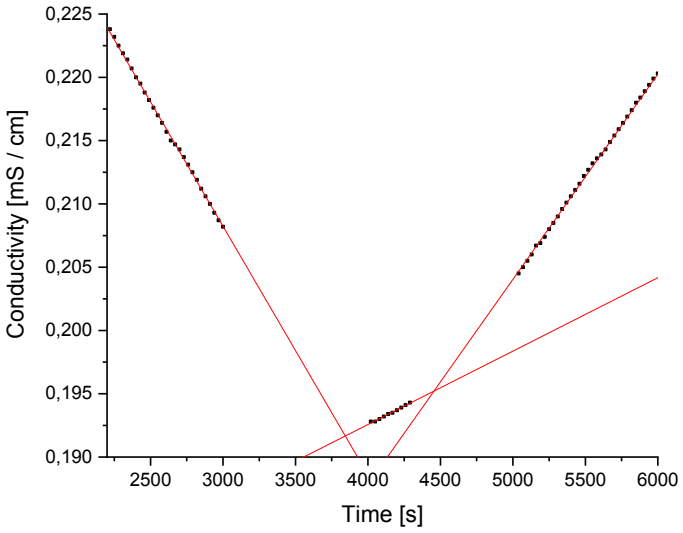

a)

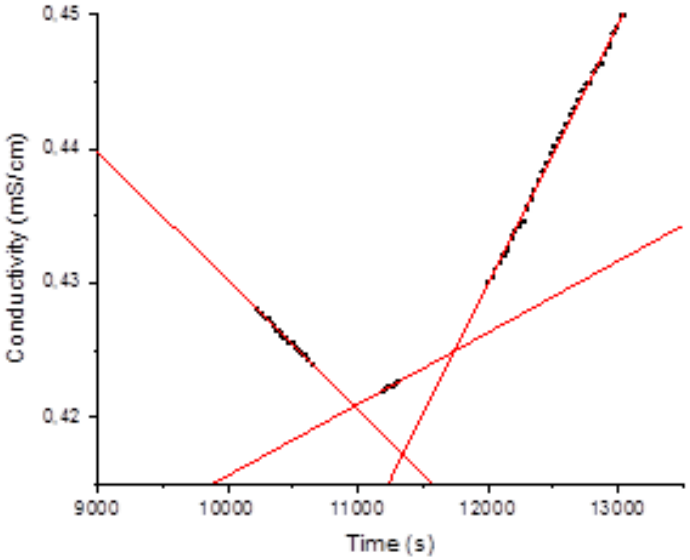

b)

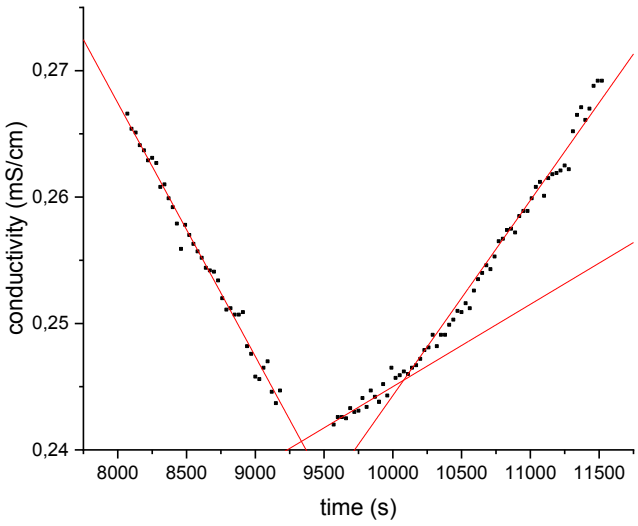

c)

Figure 11. Conductometric titration graphs: a) PCNC, batch 23418, sample dry mass 0.204 g; b) PCNC, batch 13818, sample dry mass 0.206 g and c) PCNC, batch 251018, sample dry mass 0.218 g.

The surface charge of the PCNCs in this study was found to be slightly higher than in previous studies: 11 mmol/kg cellulose for PCNCs prepared with same acid concertation and reaction time and 10-44 mmol/kg cellulose depending on PCNCs preparation conditions [81], [82]. The variance in the determined phosphorus content for different PCNC batches and the discrepancy in current and previous

studies arise, probably, due to the irreproducible nature of PCNCs preparation process. Thus, in order to exclude variance between PCNC batches, additional purification step can be recommended, for example, by extensive centrifugation, dialysis, ultrafiltration, Soxhlet extraction and/or ion exchange (or combination of these) as discussed in the studies [103]–[105].

Furthermore, as a possible reason of the observed discrepancy might be the measuring method employed for surface charge determination. The measuring method might lack reproducibility of sample preparation and full protonation of the surface moieties; and the accuracy of determination of small values of surface charge concentration. Typically, similar conductometric titration method is used for higher surface charges determination [106]. However, despite the slight disagreement with the two previous studies for PCNCS, the determined values are in reasonable agreement in comparison with previous studies for SCNCs found to be 2 - 10 times more than PCNC dimensions (see e.g. [106], [107]).

The morphology and the size distribution of cellulose nanocrystals were investigated using AFM. Individual rod-like shaped PCNCs can be observed from the obtained images (Figure 12 and 13).

a)

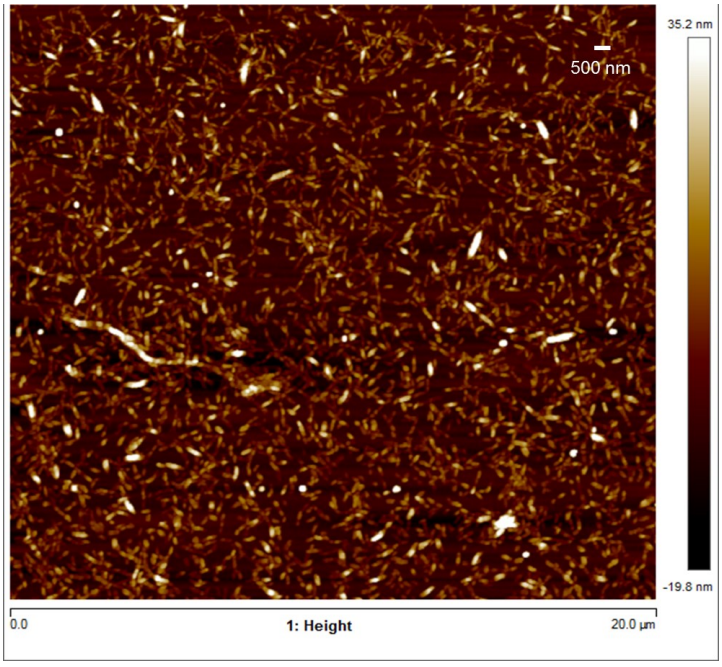

b)

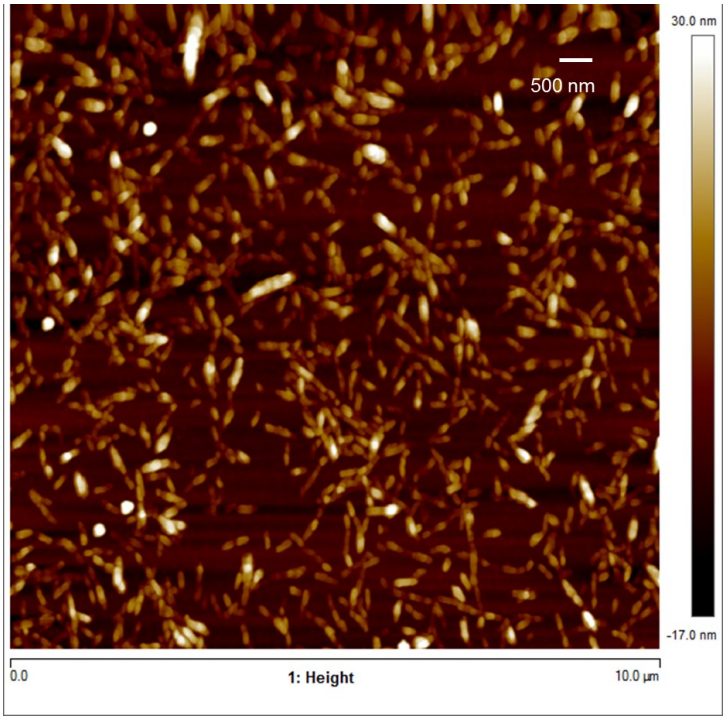

c)

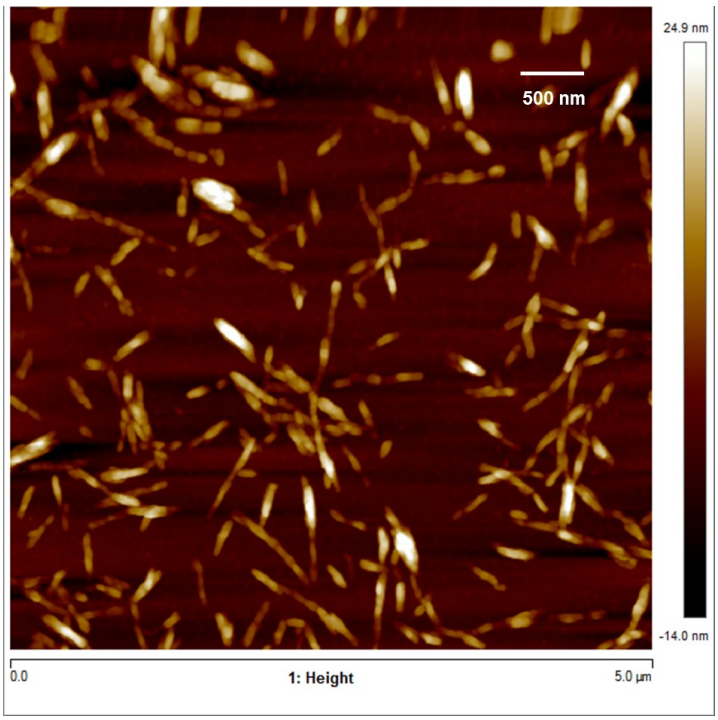

Figure 12. AFM images, showing individual PCNCs (batch 251018): a) 20x20 μm^2 surface area, b) 10x10 μm^2 surface area and c) 5x5 μm^2 surface area.

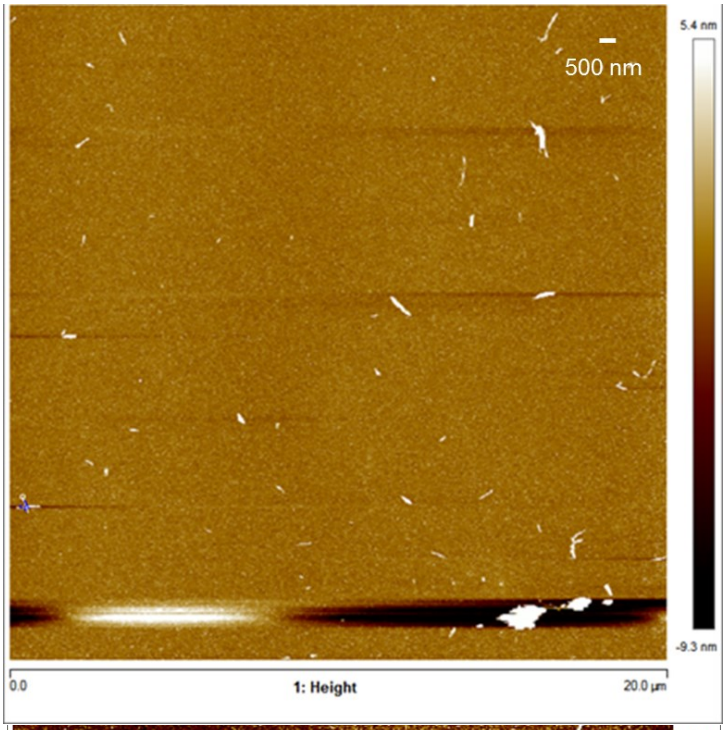
500 nm
5.4 nm
-9.3 nm
0.0
1: Height
20.0 µm

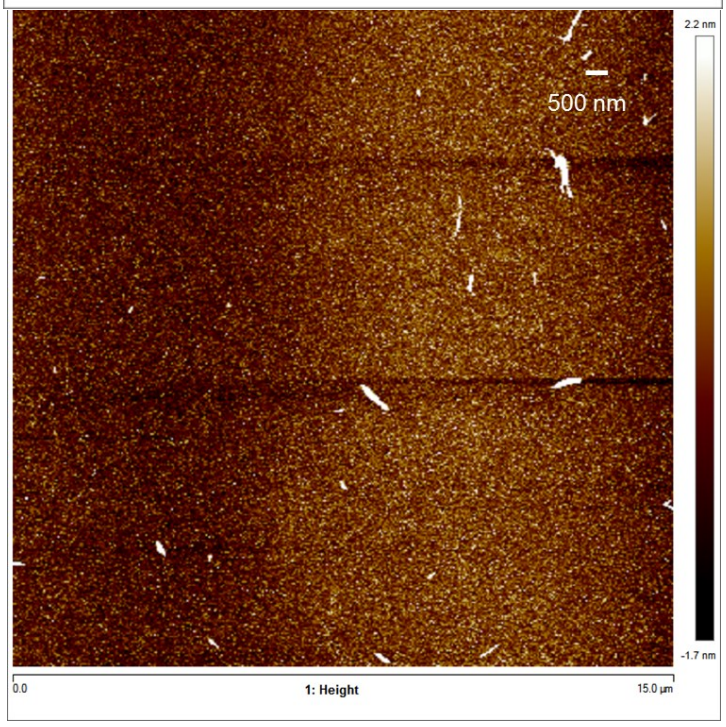
500 nm
2.2 nm
-1.7 nm
0.0
1: Height
15.0 µm

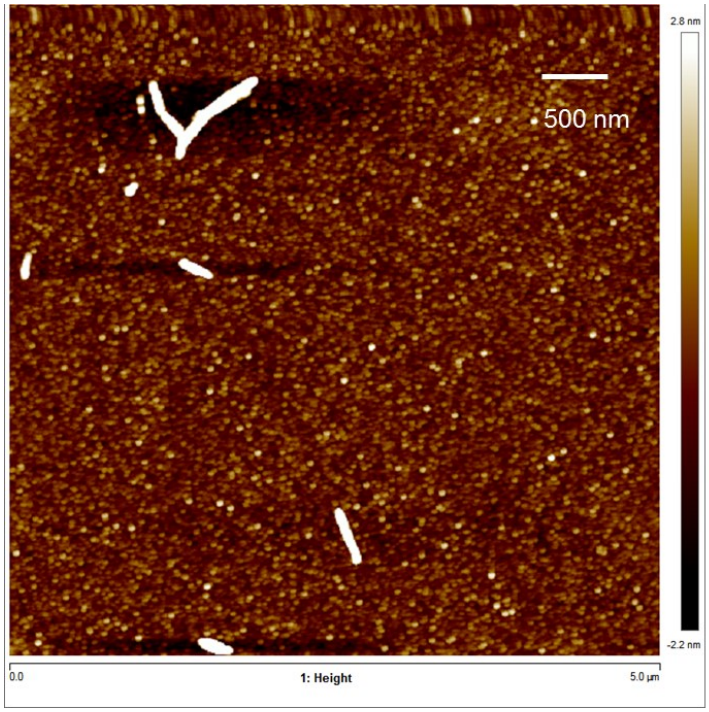

Figure 13. AFM images, showing individual PCNCs (batch 13818): a) 20x20 μm^2 surface area, b) 15x15 μm^2 surface area and c) 5x5 μm^2 surface area.

However, the distribution of the PCNCs on the TiO_2-covered wafers was not uniform, and on the AFM images one can observe some aggregations of the nanocrystals. The dimensions of the individual rod-shaped nanocrystals were measured manually from AFM images. Considering the individual nanoparticles from the AFM images, the mean values of the length (L) and diameter (D) of the isolated PCNCs (batch 251018) were determined to be 225 (± 59) nm and 11 nm (± 3) nm respectively. For the batch 138181 average particle length was determined 256 (± 88) nm and average particle diameter 13 (± 8) nm. The estimated dimensions of PCNCs in the research agrees qualitatively with the previous studies [81], [82].

Liquid-state NMR analysis did not show the presence of phosphate esters in PCNCs and modified PCNCs (Figure 14). Phosphate esters are known to be below the detection limit, however, the method is used for determination of most common phosphorus groups [108], and it was expected to detect the presence of phosphate esters. Absence of phosphate esters in PCNCs samples could be explained by preparation process of PCNCs sample for Liquid-State NMR analysis, when the phosphate esters might cleave off during the dissolution process of PCNCs samples.

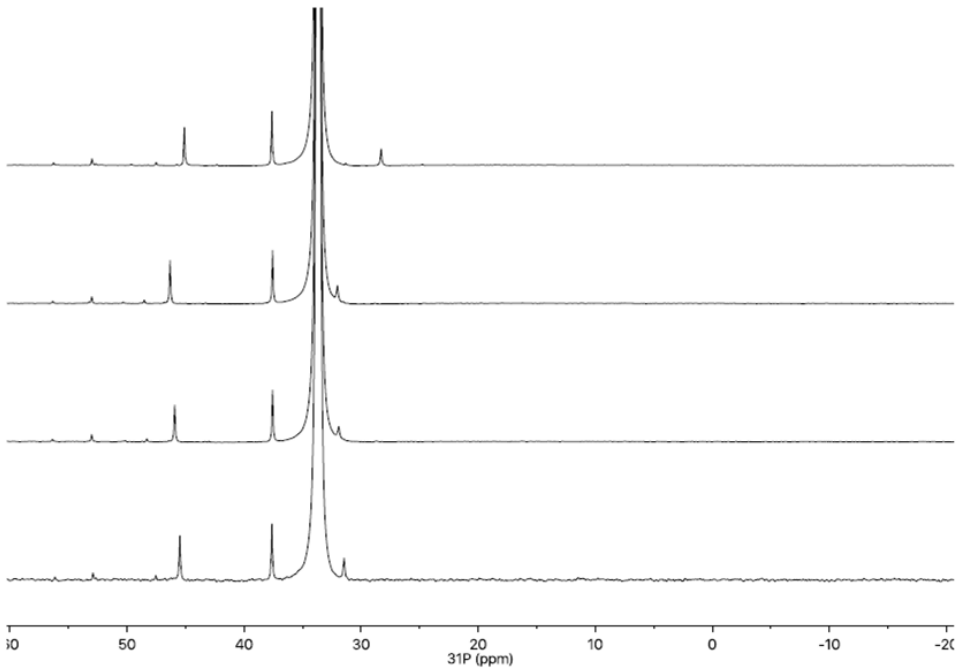

Figure 14. The 1D ^{31}Phosphorus NMR spectra for the modified and pristine PCNCs (phosphate esters are not observed around 0 ppm).

During the thesis work, three batches of PCNCs were prepared, which is not sufficient for generalizing the data. Nonetheless, trends can be observed for prepared PCNCs in this study: individual rod-like shaped nanocrystals with surface charge between 55 and 80 mmol/kg and with average length 225 or 256 nm and diameter 11 or 13 nm have been produced, resulting in an aspect ratio of ca. 20. PCNC preparation procedure appears to lack the reproducibility, having a variance between prepared PCNC bathes as it was discussed above.

CNCs preparation and dispersion state of HCNCs, SCNCs and PCNCs in methacrylate-based matrix

Three types of CNCs were prepared in the study: SCNCs, HCNCs, PCNCs. Examples of pre-tests for evaluating the dispersion of HCNCs, SCNCs and PCNCs in a resin matrix at concentration 5 wt.% are presented in Figure 15.

a) 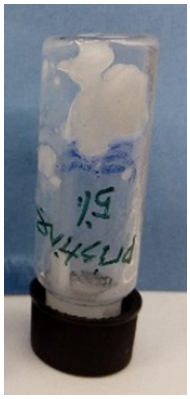 b)  c) 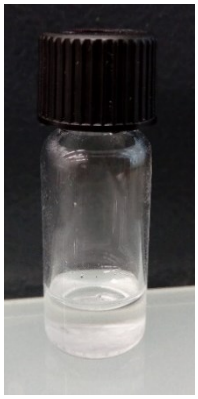

Figure 15. Comparison of dispersion of HCNC, SCNC and PCNC in HEMA/TEGDMA (80/20,v/v): a) 5 wt.% SCNC, b) 5 wt.% PCNC and c) 5 wt.% HCNC)

HCNCs were not able to disperse in the co-monomer solution: the particles stayed undispersed as a visible sediment, as HCNC are known to have very limited ability to disperse [70] and it was expected. Compared to HCNCs, better suspension was obtained for SCNCs. However, the dispersion of SCNCs in HEMA/TEGDMA solution was still very poor. Visible by naked eye, undispersed flocks were observed in monomer solution with 5 wt.% of SNCNs. Monomer solutions with less than 5 wt.% concentration of SCNCS quickly sedimented. PCNCs dispersed in the co-monomer solution better than the other unmodified CNC grades: without visible flocks and aggregates, forming a stable homogeneous mixture with the resin. Higher than 7 wt.% concentration of PCNCs caused a formation of visible agglomerates. In further studies 7 wt.% was, therefore, used as the maximum concentration for PCNCs in the resin matrix.

4.2. Characterization of modified CNCs

FTIR analysis was used to verify the modification of CNCs by different methods. Modification of CNCs with MPS can be proven by the appearance of new bands compared to pristine CNCs: peaks attributed to specific Si bonds (Si-O-Si, Si-O-cellulose), C =O and C=C double bonds from MPS as denoted in Figure 10.

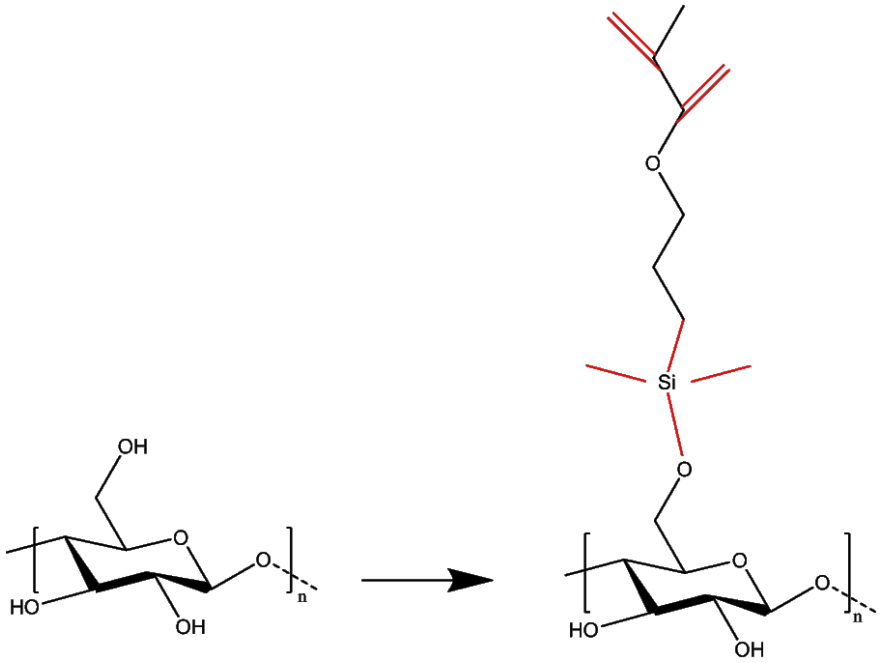

Figure 16. Modified CNC: new bonds in red colour are used for analysis.

Table 5 summaries characteristic group frequencies used for assessment of the CNC silylation.

Table 5. Summary of characteristic group frequencies used for assessment for the CNC silylation.

Chemical bond	Absorbance peak, cm^{-1}	Reference
Si-C, Si-O	760	[91]
Si-O-Si	1040	[109], [110]
–Si–O–Si–	1135	[109], [110]
–Si–O–Cellulose	1200	[109]
C=C	1637	[109], [110]
C=O	1712	[109], [110]
C=O	1720	[88], [109], [110]

Figure 17 presents the FTIR spectra of modified HCNC at different conditions in comparison with pristine HCNC.

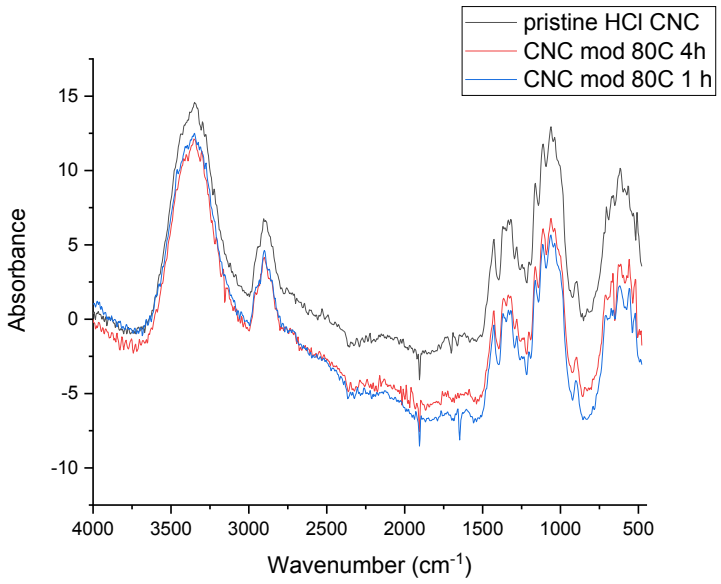

a)

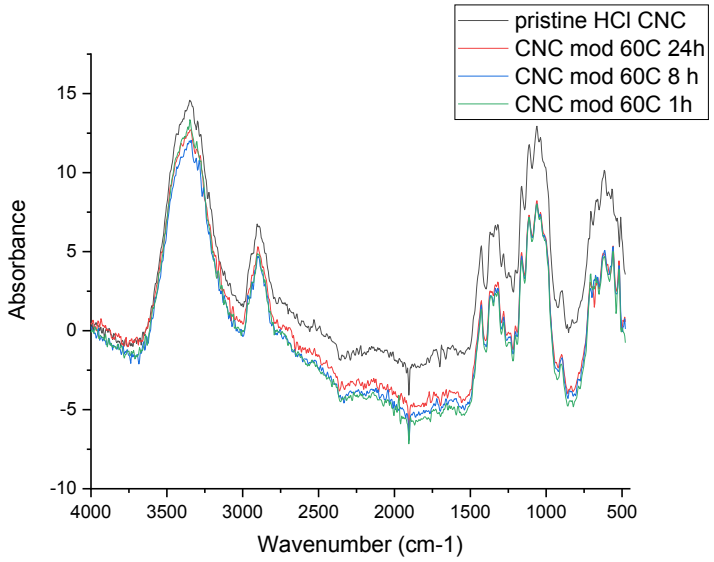

b)

Figure 17. IR spectra of modified HCNCs in comparison with pristine HCNC: a) mHCNC_80/1 and mHCNC_80/4 and b) mHCNC_60/1, mHCNC_60/8 and mHCNC_60/24.

Similar spectra of modified and pristine samples indicate that modification of HCNC performed by CVD was not successfully achieved and the chosen experimental conditions (time and temperature) for CVD reactions were not sufficient to

chemically modify HCNCs. The explanation could be found in the fact that during the experiment, the silicon compound, probably, condensed or adsorbed on the HCNCs surface. However, the layer of silane compound has not formed covalent bonds with the hydroxyl groups, and it was likely removed during the purification step.

Figure 18 presents IR spectra of modified SCNCs in comparison with pristine SCNCs.

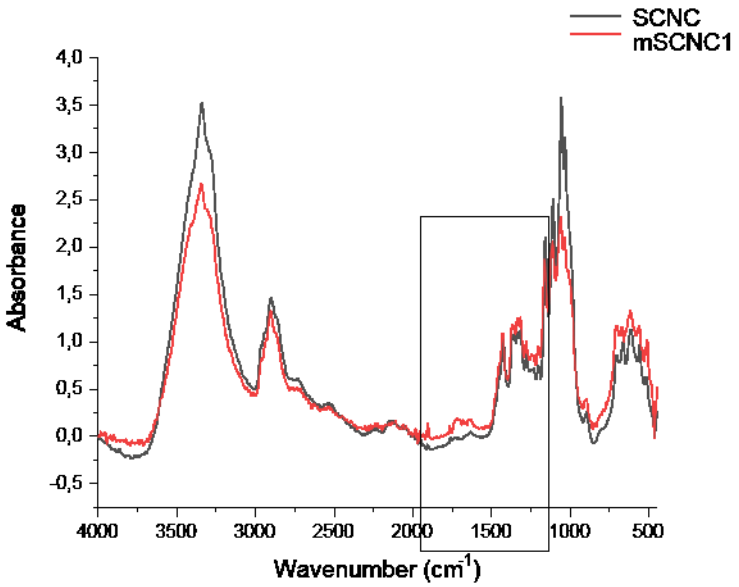

a)

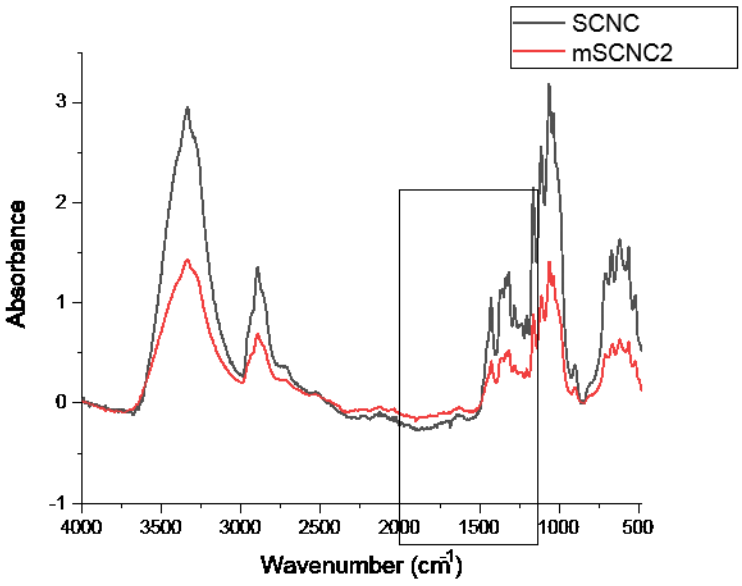

b)

Figure 18. IR spectra of modified SCNCs compared with pristine SCNCs: a) mSCNC1 and b) mSCNC2.

The appearance of new peaks at the fingerprint region has not observed for the both mSCNC1 and mSCNC2 samples compared to pristine ones, indicating the absence of specific bands corresponding to Si-O-Si and Si-O- cellulose. Bands coming from cellulosic material might overlap those bands. However, new peaks attributed to C=O or/and C=C groups cannot be detected in the spectrum either, suggesting that the modification of SCNCs was not successful. The reason for that might be the sulphate groups present on the SCNC surface and/or residual acid left from hydrolysis reaction, which interfered the silylation reaction. Another possible reason for the failure to modify SCNCS might be reduced accessibility of SCNCs hydroxyl groups due to present sulphate half ester groups on their surface. [105]

Since no evidence on the success of the performed modification reactions in HCNCs and SCNCs were observed, therefore these CNC types were excluded from the next stage of the research work.

Figure 19 shows IR spectra of modified PCNCs in comparison with pristine PCNCs: mPCNC1 (Figure 19a) and mPCNC2 (Figure 19b).

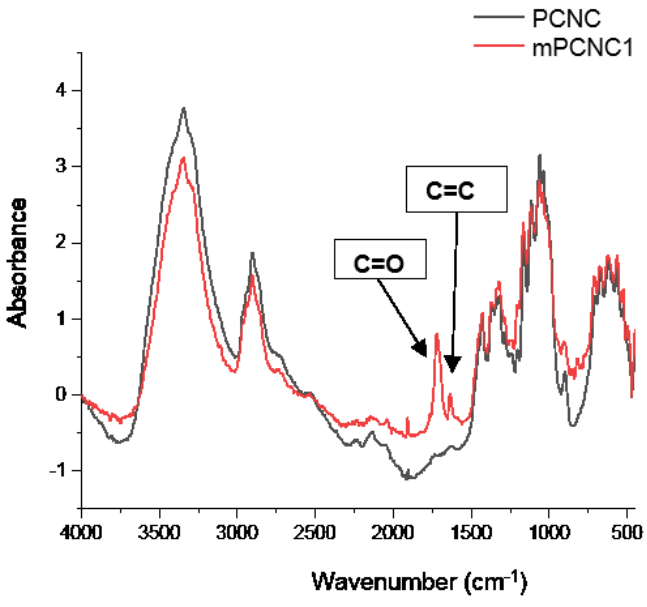

a)

b)

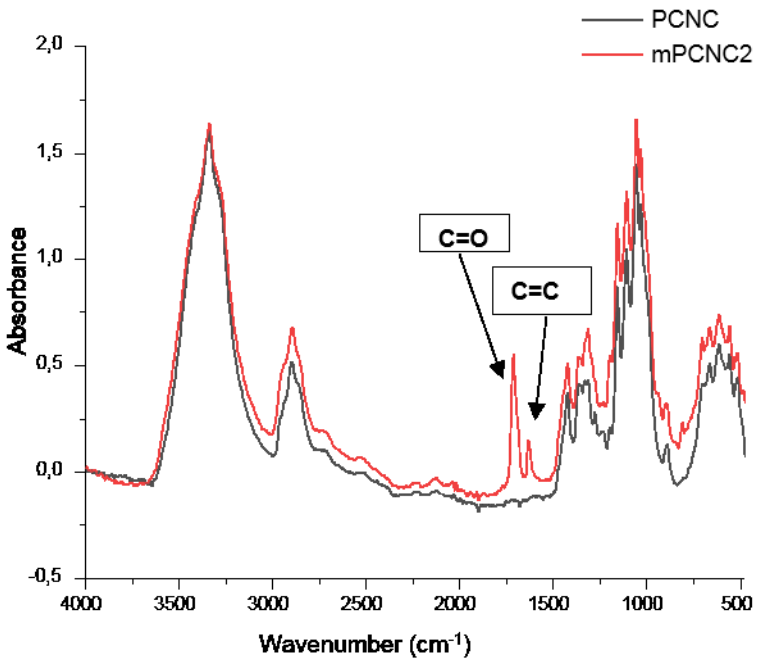

Figure 19. IR spectra of modified PCNCs compared with pristine PCNCs: a) mPCNC1 and b) mPCNC2.

On the obtained spectra for the mPCNC1 and mPCNC2 in comparison with reference pristine PCNC sample can be observed an absence of Si-O-Si and Si-O-cellulose signals, which might confirm covalent modification of PCNCs. However, the appearence of two strong peaks at region 1610-1750 cm^{-1} obviously reveals successful modification: a new peak at 1712 cm^{-1} is attributed to C=C functional group, and a new peak near 1629 cm^{-1} - to C=O group. New peaks on IR spectra of both mPCNC1 and mPCNC2 samples compared to reference, show the presence of functional groups from MPS on the PCNCs surface. These peak assignments are in agreement with those reported in other studies dealing the similar modifications of cellulose with the same silane coupling agents [88], [109], [110].

In order to confirm the interpretation of PCNC modification by FTIR analysis, both mPCNC1 and mPCNC2 were further characterized by Liquid-State NMR. The silylation reaction was confirmed by Liquid-State ^{1}H NMR. Both obtained spectra for mPCNC1 (Figure 20a) and mPCNC2 (figure 21a) confirmed the presence of cellulose anhydroglucose unit, siloxane and methacrylate groups. However, from the

diffusion-edited ^{1}H spectra (Figure 22), one can evidently observe the difference between the mPCNC1 and mPCNC2: resonance peaks in the range 1 to 2, around 4 and in the range 5 to 6 ppm, corresponding to the groups in siloxane compound are presented on the obtained spectra for mPCNC1. The extractions of the siloxanes of the surface of the mPCNC1 and mPCNC2, with both DMSO-d_6 and CD_3OD, further confirmed the difference in modification by two methods (Figure 23). Significantly more soluble siloxanes in mPCNC2, compared to that in mPCNC1 indicated that only a trace amount of silane compound has been covalently attached to mPCNC2.

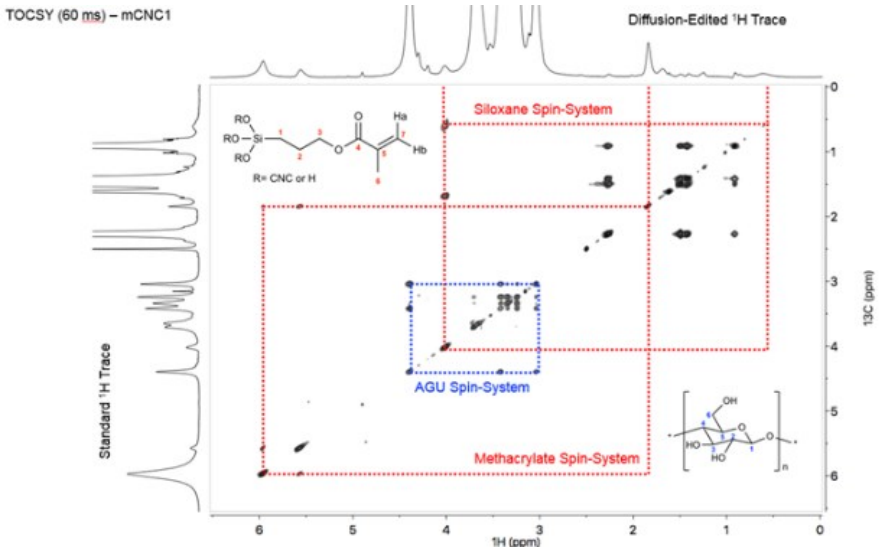

a)

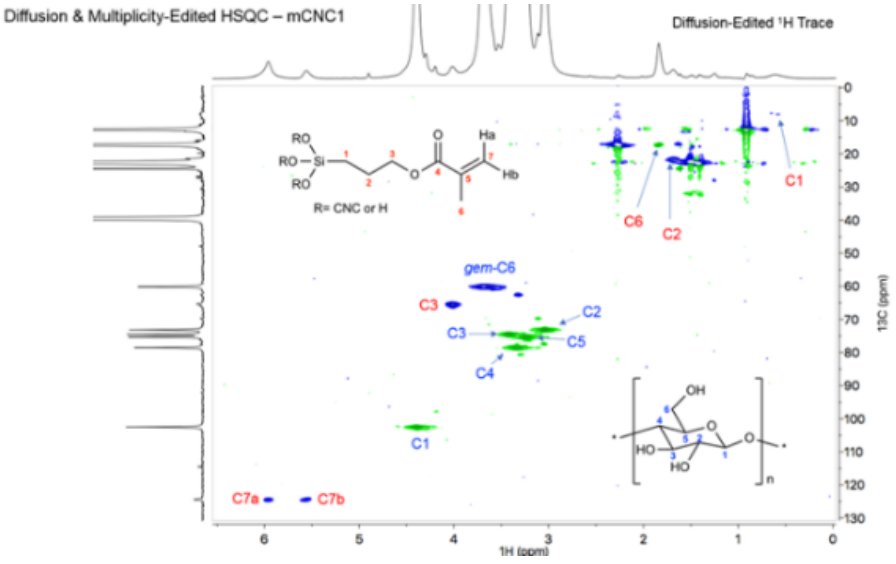

b)

Figure 20. Liquid-state NMR for modified mPCNC1: a) Diffusion-edited HSCQ spectra for mPCNC1 with resolution regions: cellulose anhydroglucose unit, siloxane and methacrylate groups; b) Multiplicity-edited HSCQ spectrum.

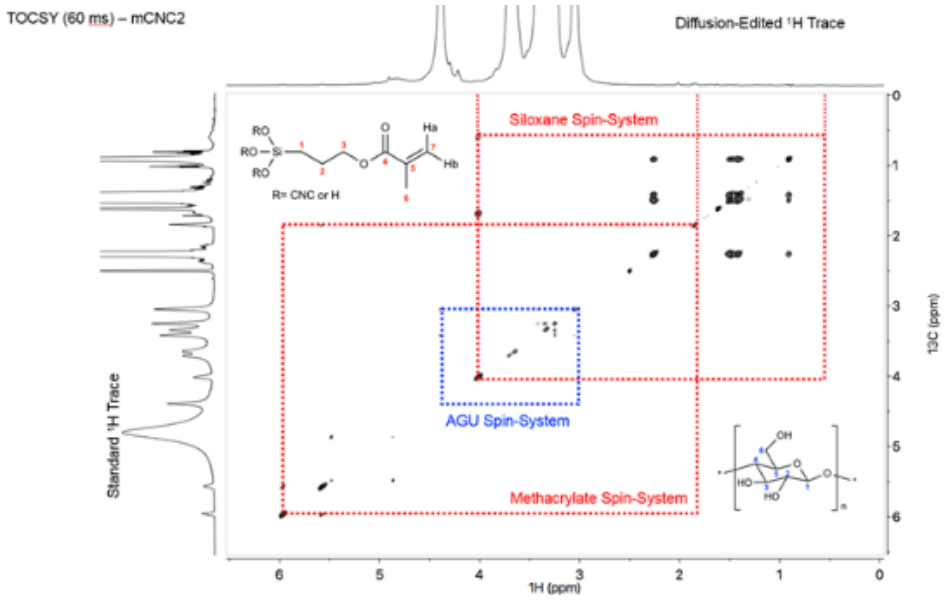

a)

b)

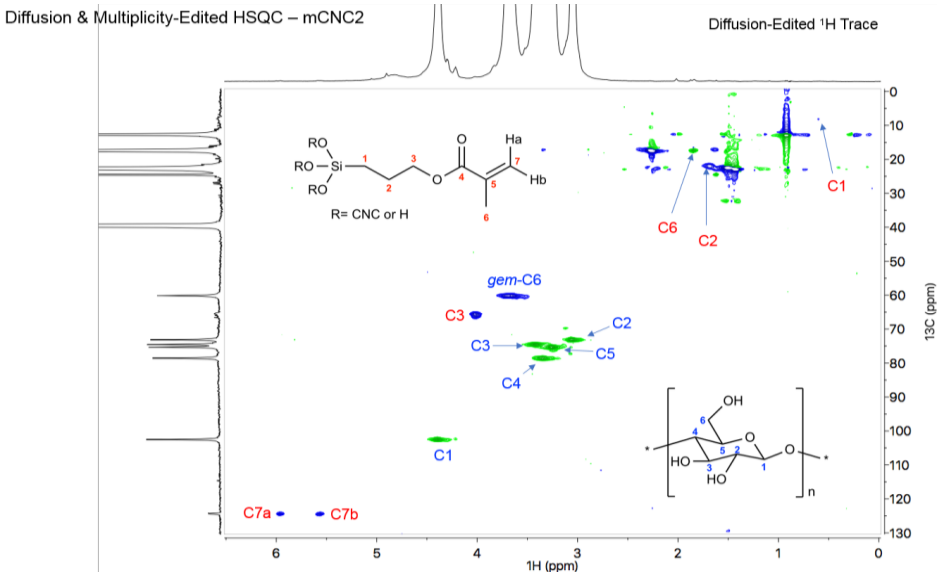

Figure 21. Liquid-state NMR for modified mPCNC2: a) Diffusion-edited HSCQ spectra for mPCNC2 with resolution regions: cellulose anhydroglucose unit, siloxane and methacrylate groups; b) Multiplicity-edited HSCQ spectrum.

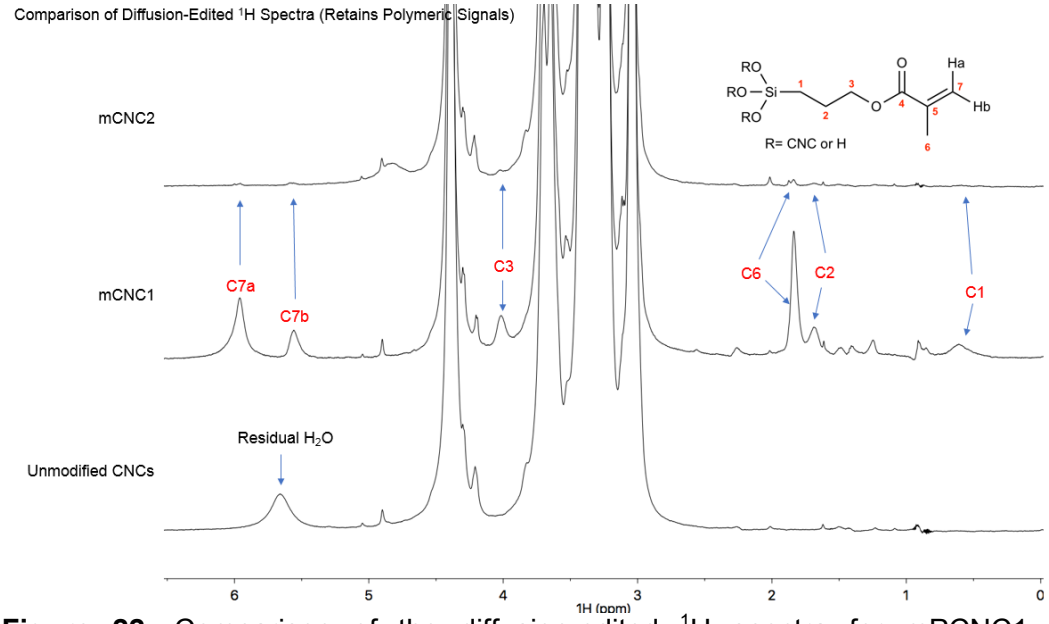

Figure 22. Comparison of the diffusion-edited ^{1}H spectra for mPCNC1 and mPCNC2 and pristine PCNCs.

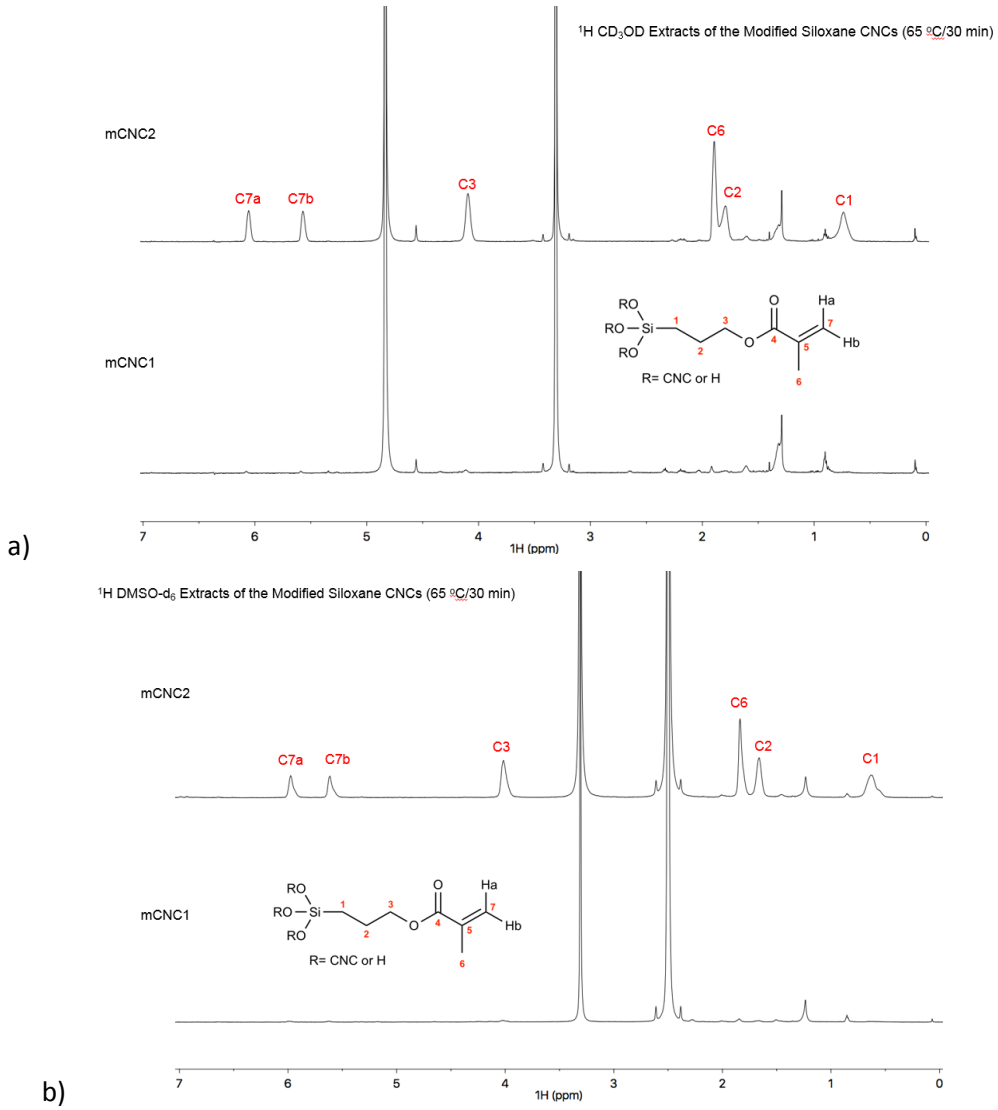

Figure 23. Liquid-state NMR spectra of extractions of the siloxanes for mPCNC1 and mPCNC2: a) extractions of the siloxanes with CD_3OD at 65° C for 30 minutes and b) extractions of the siloxanes with DMSO-d_6 at 65° C for 30 minutes.

4.3. Nanocomposite characterization

4.3.1. Degree of monomer conversion

The effect of inclusion of PCNC and mPCNC2 on the degree of conversion was evaluated on an example of the nanocomposites with bisGMA/TEGDMA matrix. Figure 24 plots the results of real-time IR study of the prepared samples based on bisGMA/TEGDMA co-monomer solution with 1 wt.% and 3 wt.% of PCNC and mPCNC2.

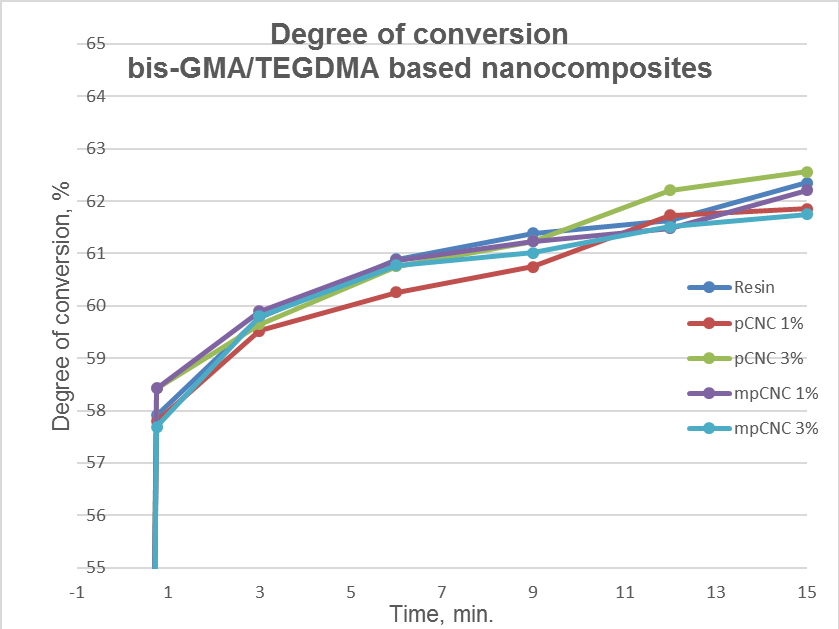

Figure 24. Degree of conversion of the nanocomposites with 1 wt.% and 3 wt.% PCNC and mPCNC2 in bisGMA/TEGDMA matrix.

No significant differences in the conversion kinetics among the samples with included PCNC and mPCNC2 were found. All samples reached 58% degree of conversion after 45 seconds irradiation and 62% after 15 minutes. The values show the same trend as reported previously (see e.g. [98]) with the typical degree of conversion for dimethacrylate polymers ranges between 43% and 75%. Thus, based on the tests, it can be concluded, that the inclusion of PCNC or mPCNC2 does not affect the kinetics of the polymerization.

4.3.2. Mechanical Properties

The nanocomposite samples were prepared out of two model resin mixtures and CNCs (PCNC and mPCNC2), and out of them bar-shaped specimen (25 mm length, 2 mm thickness and 2 mm height) were fabricated for Flexural strength test. The effect of weight fraction of the PCNCs and mPCNC2 on the nanocomposites mechanical properties and structure was studied. For both polymeric matrices, resin samples without PCNCs were prepared as control references for this study.

Samples of HEMA/TEGDMA-based nanocomposites with 1, 3, 5 and 7 wt.% of PCNCs (batch 23418) and 1, 3 and 5 wt.% of mPCNC2 (batch 251018) in comparison with resin reference are presented in Figure 25 (sample with 7 wt.% PCNCs is missing in the figure). Specimens with 7 wt.% of PCNCs for Flexural strength test were the most difficult to prepare due the increasing viscosity of the liquid samples in combination with a small working area of the mould, which created an increased risk of making structural defects. Due to the fact that the samples with 7 wt.% of mPCNC2 were too viscous, specimens for mechanical testing out of it were not prepared.

The produced polymeric specimens were glossy and transparent, with a distinct yellow tint obtained from the initiator. Addition of PCNCs into resin matrix affected positively, by promoting discoloration of the specimens and vanishing of gloss, resulting in a dental adhesive, better matching with the natural teeth colour.

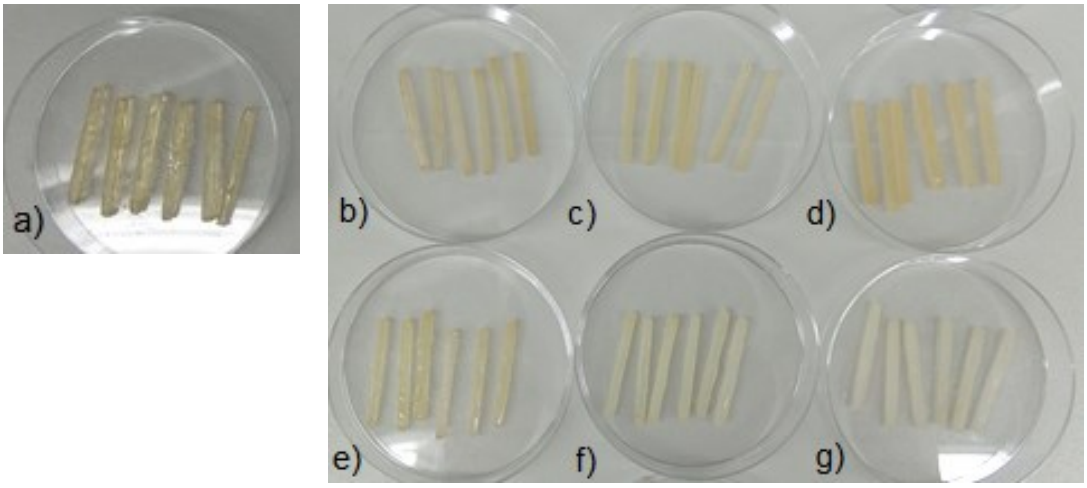

Figure 25. Flexural strength test specimen: a) resin reference, b) 1 wt.% PCNC containing sample, c) 3 wt.% PCNC containing sample, d) 5 wt.% PCNC containing sample, e) 1 wt.% mPCNC2 containing sample, f) 3 wt.% mPCNC2 containing sample and g) 5 wt.% mPCNC2 containing sample.

Samples of co-monomer solution bisGMA/TEGDMA with 1 wt.% and 3 wt.% of PCNCs and mPCNC2 were prepared, and specimens for mechanical testing were manufactured out the samples for the study.

The results of Flexural strength tests are presented in Table A1 for the HEMA/TEGDMA-based samples in Appendix 1. Figure 26 plots flexural strength of the nanocomposites (HEMA/TEGDMA matrix) in comparison with the results of reference resin HEMA/TEGMA testing (for each sample presented mean value and standard deviation).

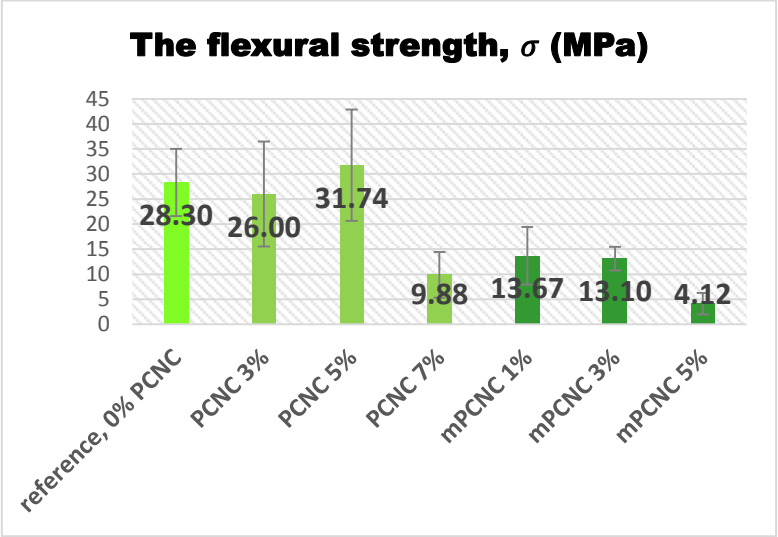

Figure 26. The flexural strength for experimental adhesives (HEMA/TEGDMA matrix) with different weight content of pristine PCNCs and mPCNC2 in comparison with resin reference (HEMA/TEGDMA matrix, 0% PCNC).

The specimens with 1 wt.% of PCNCs failed to test being too elastic. The composite sample with 3 wt.% PCNC had flexural strength value similar to that of the reference sample, and only the sample with 5 wt.% of PCNCs in HEMA/TEGDMA composition improved the mechanical properties of the nanocomposite to some extent (the mechanical performance was improved by 12% as compared to the control reference sample). The larger weight fraction of PCNCs (7 wt.%), did not further improve the mechanical properties, on the contrary, it reduced the mechanical properties of the nanocomposite similar to the study [111]. This result was expected and showed similar tendency to the previous studies [71], [78]: there is a point at which an excessive nanoparticle concentration forms large aggregate clusters and starts to influence negatively the mechanical properties of a nanocomposite.

The registered high standard deviation for all tested samples might be an indicator of problems during specimen fabrication by LED device, causing structural inner and surface defects. Among the problems, enhancing variability of the observed results, are: trapped air bubbles in specimen [112], inhomogeneous polymerization of specimens due to its bigger size compared with emitting source and use of sequential light irradiation [113], [114], and the presence of flaws at the edges of samples due to the relatively large size of the specimen [115].

The results of Flexural strength tests of the bisGMA/TEGDMA-based samples are presented in Table A2 in Appendix 1. Figure 27 plots the flexural strength of the nanocomposites (bisGMA/TEGDMA matrix) and the control reference resin bisGMA/TEGMA (for each sample presented mean value and standard deviation).

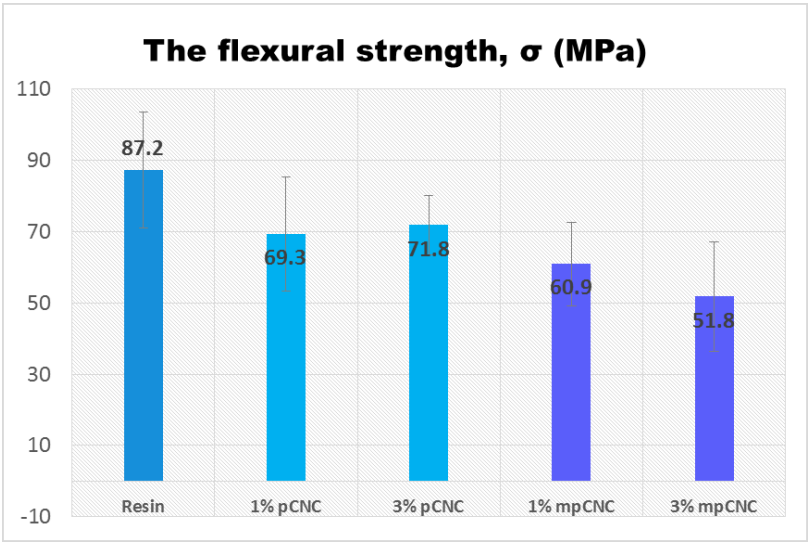

Figure 27. The flexural strength for experimental adhesives (bisGMA/TEGDMA matrix) with different weight content of pristine PCNCs and mPCNC2 in comparison with resin reference, bisGMA/TEGDMA.

The flexural strength values of the tested nanocomposite samples based on bisGMA/TEGDMA were overall significantly higher that HEMA/TEGDMA-based nanocomposites. These results were expected due to typically more viscous bisGMA resins showing better mechanical properties. However, surprisingly, inclusion of PCNCs or mPCNC2 to bisGMA/TEGDMA-based matrix reduced mechanical properties of the resulting nanocomposites. PCNCs moderately decreased the flexural strength of the nanocomposites compared to the reference

resin sample; however, mPCNC2 had a more pronounced effect on the reduction of mechanical properties. Similar results have been noticed for the HEMA/TEGDMA-based samples: mPCNC2 decreased flexural strength significantly. An explanation could be found in the reduction of the mechanical properties of mPCNC2 due to the chemical modification procedure.

4.3.3. Structural analysis of the nanocomposites

The nanocomposite structure and distribution of PCNC and mPCNC2 in HEMA/TEGDMA and bisGMA/TEGDMA-based matrices was preliminary studied by light microscopy. The unpolymerized liquid samples with 3 wt.% mPCNC2 in two methacrylate-based matrices, bisGMA/TEGDMA and HEMA/TEGDMA, in comparison to the sample containing PCNCs in bisGMA/TEGDMA matrix were chosen for examination. The light microscopy images are presented on Figure A1 in Appendix 2. Study of the morphology of the unpolymerized nanocomposites in liquid state by light microscopy revealed similar morphology of two samples with mPCNC2 - “fiber-like” uniformly distributed networks appearing as dark thin stripes on both microscopy images. However, the image presenting the sample with PCNCs, has large dark areas of different shapes that could be considered as PCNCs aggregates.

The structure and morphology of the nanocomposites was further studied on nano scale via TEM. Figure 28 presents the images of polymerized nanocomposite with 3 wt.% of PCNC and mPCNC2 in bisGMA/TEGDMA matrix, showed in varied darkness (from light grey to almost black colour), indicating the material density in different parts of the specimen.

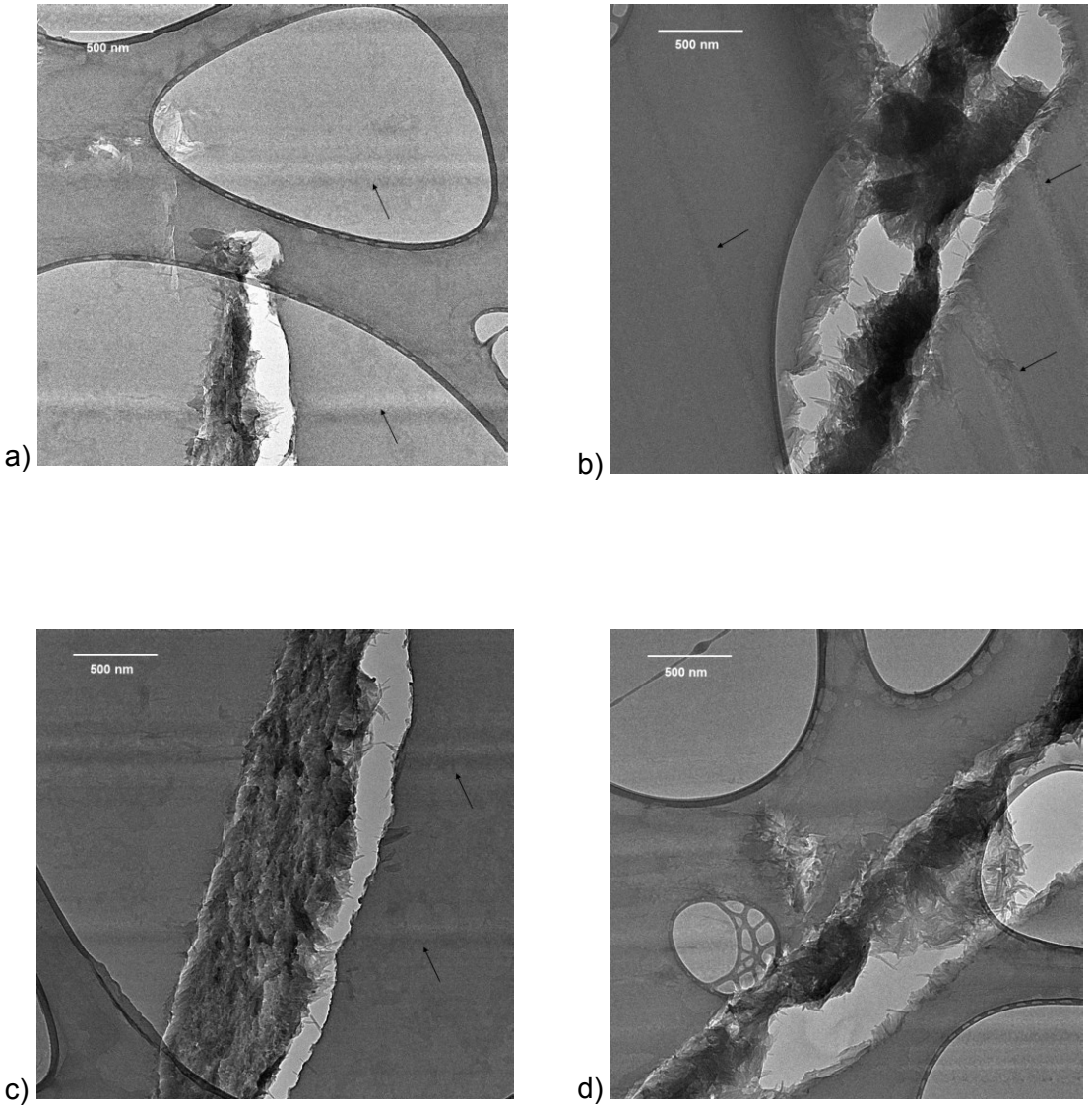

Figure 28. TEM images of the polymerized bisGMA/TEGDMA-based nanocomposites with 3 wt.% PCNC: a) individual PCNCs in the polymer matrix; b) darker areas around the crack depict vast PCNCs clusters; c) vast elongated crack with PCNCs clusters agglomerated on the long edge of the crack; d) aligned stripes across the specimen.

Study of the sample with 3 wt.% PCNCs revealed presence of insignificant amount of individual PCNCs (Figure 28a) and their agglomerates (Figure 28b,c and d), as well significant amount of cracks in the nanocomposite structure. The observed numerous elongate-shaped cracks range in length from a few hundred nm to few μm. Extensive accumulations of individual PCNCs have been found on one side of the long edge of every crack. Remarkable feature of the structure were numerous

parallel-oriented regular stripes (stripes are pointed out by arrows, see e.g. Figure 28a, b and c), they might be result of similar to presented on the images agglomerates of PCNCs in the direction, perpendicular to the sliced specimen. However, the nature of the regular parallel alignment across the specimen is unclear and requires additional study.

As shown on images (Figure 29a-d), the sample with 3 wt.% of mPCNC2 has significantly more individually dispersed mPCNC2 than the sample with PCNCs (Figure 28). Similar to the sample with mPCNC2, elongated cracks can be observed (Figure 29b and d). However, the cracks are significantly smaller. Likewise, mPCNC2 aggregates accumulated around cracks in structure similar to the previous sample are significantly smaller (compare with dark-coloured multi-layer cluster structures of the sample with pristine PCNCs on Figure 28a-d). At higher magnification (Figure 29c), individual mPCNC2, accumulated around the edge of the crack, are clearly identified. However, the obtained TEM images of mPCNC2 sample do not allow to conclude the presence of percolation network in the experimental nanocomposites.

a) 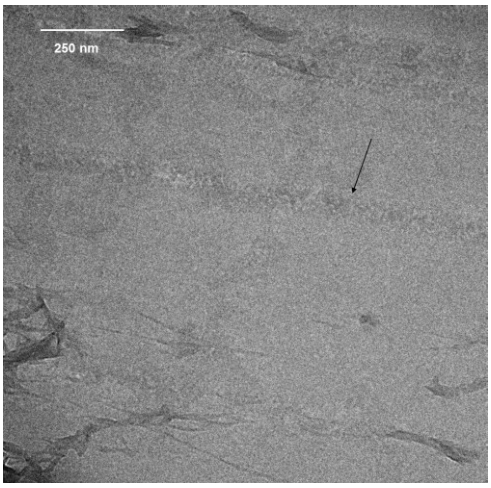

b) 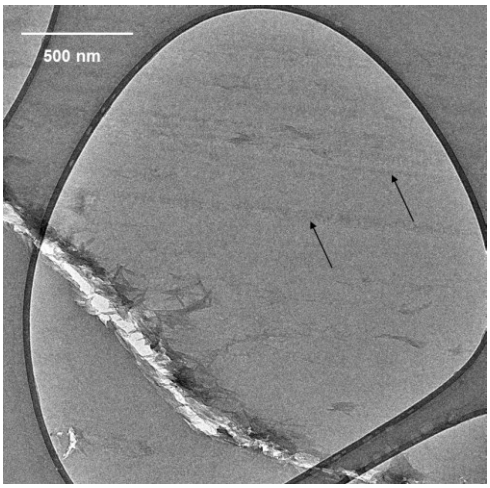

c) 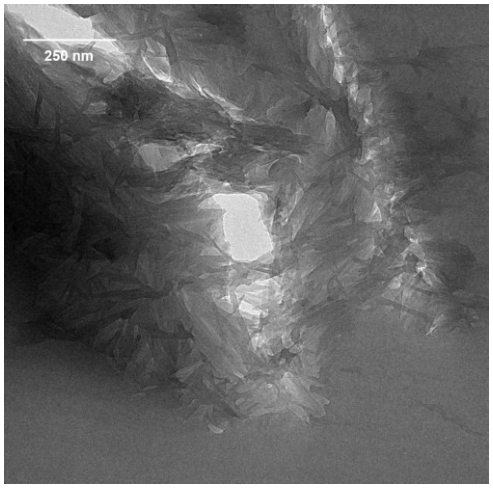

d) 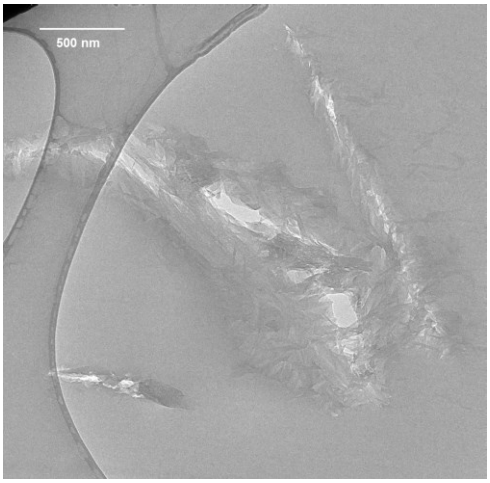

Figure 29. TEM image of the polymerized bisGMA/TEGDMA matrix with 3 wt.% mPCNC2 :a) individual mPCNC2 and elongated crack with mPCNC2 aggregates; b) agglomeration of PCNCs and cracks on the network; c) magnified agglomeration of PCNCs around hole in the nanocomposite structure and d) moderate aggregates of PCNCs around crack and aligned stripes are observed.

The study of the nanostructure of the samples revealed the fact that both PCNCs and mPCNC2 were not homogeneously dispersed in the polymer matrix. The appearance of bonded together PCNCs and consequence formation of aggregates is expected due to high specific area of CNCs and strong hydrogen bonds. The clusters of PCNCs in the nanocomposite structure could create zones, lacking co-monomer solution infiltration, which were not able to polymerize. Further, those zones could act as stress concentration areas, and hence result in the reduction of the mechanical properties of the resulting material.

TEM images of the sample with mPCNC2 allow to conclude that chemical modification of PCNCs promoted their dispersion in polymer matrix, as more individual mPCNC2 have been observed and their clusters were less extensive compared to the nanocomposites with pristine PCNCs. The appearance of vinyl bonds on mPCNC2 surface as a result of silylation, contributed to co-polymerization reaction, as it was presented previously on Figure 3 (subchapter 2.3.3. CNCs modification and inclusion in a composite matrix). Thus, less cracked zones are observed on TEM images of the mPCNC2 containing sample. However, the

homogenous dispersion of mPCNC2 is not observed similar to the other attempts to disperse CNCs in polymer matrix [116].

The relation between evaluated mechanical properties of the nanocomposites and their nanostructure is not obvious: despite the observed on TEM images better dispersion of mPCNC2 compare to PCNCs, the samples with mPCNC2 showed reduction of flexural strength of the nanocomposite samples with 1 – 3 wt.%. One of the possible reasons might be the overall reduction of the mechanical properties of individual mPCNC2 due to performed modification reaction. However, the relationship between the mechanical testing and morphological observations has controversial nature and careful and systematic investigation is necessary. Thus, the samples with various PCNC and mPCNC2 content with HEMA-based matrix are lacking morphological study.

5. Conclusion

The work aimed to develop a novel dental adhesive, providing durable and long-lasting bonds. During this work, the researcher explored the possibility of application of three different types of nanocellulose into two light-polymerized methacrylate-based matrices. Within the limited framework of the Master's thesis, the main task - development of a novel dental adhesive, is incomplete. However, the work narrows down possible alternatives and finds the suitable component for a dental adhesive and points out the direction for the further product development.

Based on the results of the study, from the three types of CNCs studied in the project, PCNCs were found to be the most favourable component for the dental adhesives. Both pristine and modified PCNCs were able to disperse in two experimental co-monomer matrices. In the polymerized samples, for low viscous methacrylate-based matrix, such as HEMA/TEGDMA matrix used in the study, PCNCs were able to improve flexural strength, acting as a reinforcement component (inclusion of 5 wt.% PCNCs contributed to improvement of flexural strength by 12%). However, as the prepared nanocomposite still does not have mechanical strength sufficient enough to resist the oral stresses further investigations are necessary. For the more viscous matrix, bisGMA/TEGDMA polymeric matrix, PCNCs showed the potential to increase compatibility with the hydrophilic dentin tissue without significantly reducing the mechanical properties and without affecting the degree of conversion of the resulting material.

From the contradictory character of the results obtained from Flexural strength testing, the fact that only one of the nanocomposite samples had improved flexural strength and high variability within the obtained results, can be concluded the necessity of finding a proper way to prepare specimen and/or finding other test methods to evaluate the mechanical properties of experimental dental adhesives.

The modification of PCNCs was attempted through two different approaches (Method 1 and Method 2). Within the limitations of this study, only functionalized mPCNC2, obtained by the newly developed silanization protocol, (called in the study Method 2) [91], have been used in the nanocomposite preparation, which show a

decreased flexural strength for both polymer matrices in comparison to nanocomposites with pristine PCNCs. However, morphological study revealed the fact of improved dispersability and co-polymerization with methacrylate-based matrix was observed for the silylated PCNCs. Therefore, the modification by Method 1 [88], could be potentially more favorable for the nanocomposite preparation, this should be investigated.

The study has shown, that PCNCs up to 5 wt.% are possible to add *in situ* to a suspension polymerization of HEMA/TEGDMA and bisGMA/TEGDMA solutions. In fact, it was impossible to prepare homogenous samples with a concentration higher than 5 wt.% without adding solvents. Degree of monomer conversion, an important parameter of a dental adhesive, was not affected by PCNCs and mPCNC2 incorporation. Both PCNCs and mPCNC2 can be included into dental resin composition without affecting on degree of conversion. PCNCs and mPCNC2 incorporation into HEMA/TEGDMA resin did not affect neither the curing reaction kinetics, nor the degree of conversion of the resulting nanocomposite.

Among limitations of this study is the isolation process for PCNCs. The phosphoric acid hydrolysis process was used simply as described in literature [81]. Since it is a model process, yielding 1.5 to 1.8 g of PCNCs from a certain batch, several batches were prepared during the research as the sheer amount of material was necessary for the trial tests and characterization. Some optimization was introduced during the project, despite that main purpose of the research work was the preparation of a dental adhesive. Furthermore, it was noticed that each batch of PCNCs varied with its characteristics, such as dimensions, aspect ratio and surface charge, indicated the necessity of developing a reproducible phosphoric acid hydrolysis. For example, the studies has proved [105] , that for the sulphuric acid hydrolysis Soxhlet extraction step has a significant effect on the batch reproducibility of further reactions on the CNC surface after the CNC preparation. Thus, Soxhlet extraction with ethanol for the phosphoric acid hydrolysis could possibly be introduced.

Another limitation of this study is that only flexural strength and degree of monomer conversion of the experimental nanocomposites were assessed. The clinical application of a dental material requires a good knowledge about its different biomechanical properties. Other important properties for dental adhesives include

surface hardness, water sorption behavior, bond strength as a function of PCNCs mass fraction in a simulated oral environment, and biocompatibility. Those characteristics have not been evaluated, yet.

5.1. Outlook and recommendations

The research has provided fruitful information on further development of dental adhesives containing nanocellulose. There are several lines of research, arising from this work, which could be further investigated. Research suggestion for an experimental dental adhesive development is presented on the Figure 30 in a form of flowchart.

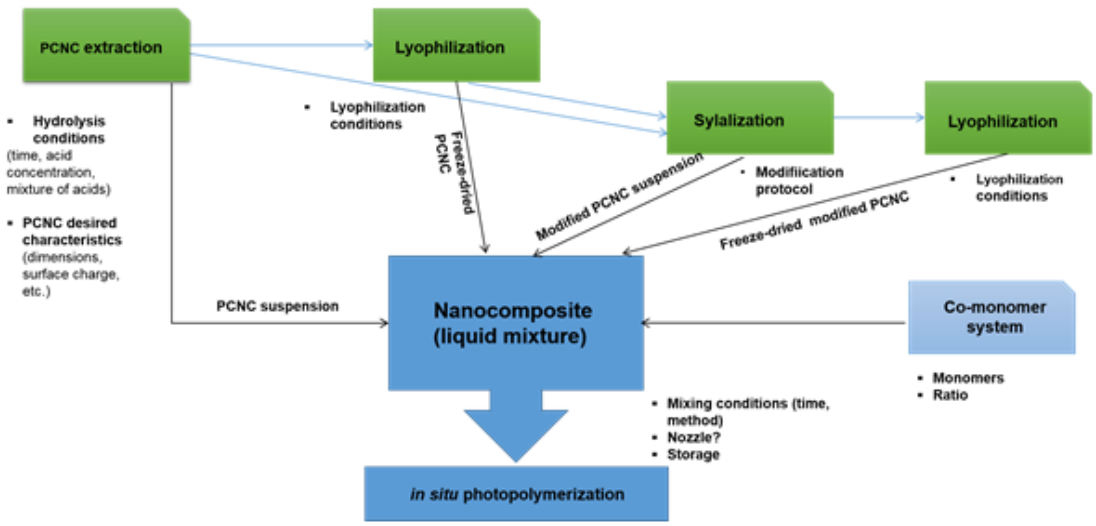

Figure 30. Schematic representation of possible lines for future research for a dental adhesive development.

1. Optimization of the phosphoric acid hydrolysis process and preparation of PCNCs on a microstructural level via different drying techniques for achieving good dispersibility in a co-monomer solution.

Preparation process of PCNCs might be developed further, yielding a reasonable amount of PCNCs from each batch, enough for characterization and preparation of

nanocomposites. Importantly, the acid hydrolysis process should be tailored reproducible, so that it produces consistent PCNCs with certain desired characteristics. Moreover, for effective isolation, a mixed acid system can be proposed for the PCNCs production [117]. Along with the hydrolysis conditions, conditions of PCNC treatment following acid hydrolysis, such as sonication and purification, impacting also its properties and behavior, could be studied further [107]. The biological source of cellulose for the process might be reconsidered as well, and alternative sources of cellulose could be suggested for the phosphoric acid hydrolysis.

Besides that, it is important to determine the crucial parameters, necessary to measure and evaluate which guarantee a consistent production of PCNCs prior to PCNC use [107]. PCNCs could be produced with desired dimensions and phosphate content depending on the polymer matrix. Thus, for reinforcing HEMA matrix PCNCs with high aspect ratio are preferable [118]. Longer CNCs with a higher aspect ratio are able to better reinforce nanocomposites by forming entangled structures and interacting with the polymer matrix. For the bisGMA-based matrix, PCNCs with smaller dimensions could be recommended as they tend to have better dispersibility, which is favorable for viscous matrix [84]. Optimal mass fraction of CNC should be found depending on the CNC size to keep the viscosity optimal for the dental adhesive application.

As freezing in liquid nitrogen and further freeze-drying of diluted PCNCs suspensions induces irreversible changes and aggregation of PCNCs, finding the optimal drying method prior to composite preparation is necessary for achieving homogenous dispersion of freeze-dried PCNCs in co-monomer solution, similar to the study [119].

2. Preparation of nanocomposite from a mixture of solvents.

A second line of further research is the investigation of possibility of a nanocomposite using solution mixing. Solvents, such as water, ethanol and acetone, are typically used in dental adhesive composition for the improving application process on the dentin surface as it was described in Chapter 2. Typically charged CNCs disperse well in water. Therefore, water is the most suitable processing medium for them. Mixtures of ethanol/water could be potential media as well. A possibility to disperse PCNCs in a mixture of ethanol/water could be investigated for the use with co-monomer solution. Thus, achievement of well-dispersed PCNCs in a

polymer matrix is possible without freeze-drying of PCNCs. Moreover, an approach with ethanol-wet bonding could also be feasible [10].

3. Finding a proper amount of PCNCs in a polymer matrix for creating percolated network.

The optimal proportion of PCNCs in nanocomposite composition has to be determined, depending on the initial viscosity of a model co-monomer solution and the PCNCs size. Some authors discussed that above a certain critical volume fraction (percolation threshold concept (see e.g. [77]), CNCs interconnect to create a network inside the matrix, which usually leads to a step-wise increase in some physical properties [120]. Thus, through finding the critical concentration of PCNCs in polymer matrix where PCNCs forms supportive network instead of aggregation [78], [118], [120], [121] is necessary in future studies. Moreover, a combination of PCNCs with different aspect ratio is possible [122]. The optimal proportion of PCNCs in nanocomposite composition has to be determined, depending on the initial viscosity of a model co-monomer solution and the CNCs size.

4. Investigation of other factors, affecting on dispersibility of PCNCs in the polymer matrix.

PCNCs dispersion in a co-monomer solution could be studied through changing the pH, and by using additives such as surfactants and polyelectrolytes. Moreover, the possibility of using different mechanical methods for better dispersion of PCNCs in methacrylate-based matrices has to be investigated in the future.

References

[1] D. N. S. Hon, “Cellulose: a random walk along its historical path,” *Cellulose*, vol. 1, no. 1, pp. 1–25, 1994.

[2] Y. Lu, H. L. Tekinalp, C. C. Eberle, W. Peter, A. K. Naskar, and S. Ozcan, “Nanocellulose in polymer composites and biomedical applications,” *Tappi J.*, vol. 13, no. 6, pp. 47–54, 2014.

[3] N. Lin and A. Dufresne, “Nanocellulose in biomedicine: Current status and future prospect,” *Eur. Polym. J.*, 2014.

[4] M. Jorfi and E. J. Foster, “Recent advances in nanocellulose for biomedical applications,” *Journal of Applied Polymer Science*. 2015.

[5] N. Halib, F. Perrone, M. Cemazar, B. Dapas, R. Farra, M. Abrami, G. Chiarappa, G. Forte, F. Zanconati, G. Pozzato, L. Murena, N. Fiotti, R. Lapasin, L. Cansolino, G. Grassi, and M. Grassi, “Potential applications of nanocellulose-containing materials in the biomedical field,” *Materials*. 2017.

[6] F. Li, P. Wang, M. D. Weir, A. F. Fouad, and H. H. K. Xu, “Evaluation of antibacterial and remineralizing nanocomposite and adhesive in rat tooth cavity model,” *Acta Biomater.*, 2014.

[7] G. Migliau, “Classification review of dental adhesive systems: from the IV generation to the universal type,” *Ann. Stomatol. (Roma).*, 2017.

[8] E. Kücükpinar and H.-C. Langowski, “Adhesion Aspects in Packaging,” *J. Adhes. Sci. Technol.*, vol. ahead-of-p, no. ahead-of-print, pp. 1–8, 2012.

[9] I. A. Mjör and V. V. Gordan, “Failure, repair, refurbishing and longevity of restorations.,” *Oper. Dent.*, 2002.

[10] L. Breschi, A. Mazzoni, E. De Stefano Dorigo, and M. Ferrari, “Adhesion to Intraradicular Dentin: A review,” in *Adhesion Aspects in Dentristry*, J. P. Matinlinna and K. L. Mittal, Eds. VSP, 2009, pp. 2–33.

[11] M. Peumans, P. Kanumilli, J. De Munck, K. Van Landuyt, P. Lambrechts, and B. Van Meerbeek, “Clinical effectiveness of contemporary adhesives: A systematic review of current clinical trials,” *Dental Materials*. 2005.

[12] R. M. Carvalho, L. Tjäderhane, A. P. Manso, M. R. Carrilho, and C. A. R. Carvalho, “Dentin as a bonding substrate,” *Endod. Top.*, 2009.

[13] G. W. Marshall, S. J. Marshall, J. H. Kinney, and M. Balooch, “The dentin

substrate: structure and properties related to bonding.," *J. Dent.*, 1997.

[14] M. Goldberg, A. Kulkarni, M. Young, and A. Boskey, "Dentin: structure, composition and mineralization.," *Front. Biosci. (Elite Ed).*, 2011.

[15] S. Liaqat, A. Aljabo, M. A. Khan, H. Ben Nuba, L. Bozec, P. Ashley, and A. Young, "Characterization of dentine to assess bond strength of dental composites," *Materials (Basel).*, 2015.

[16] K. Chun, H. Choi, and J. Lee, "Comparison of mechanical property and role between enamel and dentin in the human teeth.," *J. Dent. Biomech.*, 2014.

[17] S. Habelitz, S. J. Marshall, G. W. Marshall, and M. Balooch, "Mechanical properties of human dental enamel on the nanometre scale," *Arch. Oral Biol.*, 2001.

[18] J. Perdigão, "Dentin bonding-Variables related to the clinical situation and the substrate treatment," *Dent. Mater.*, 2010.

[19] C. Dawes, "What is the critical pH and why does a tooth dissolve in acid?," *J. Can. Dent. Assoc.*, 2003.

[20] C. P. Aires, A. A. Del Bel Cury, L. M. A. Tenuta, M. I. Klein, H. Koo, S. Duarte, and J. A. Cury, "Effect of starch and sucrose on dental biofilm formation and on root dentine demineralization," *Caries Res.*, 2008.

[21] J. Perdigão, "Dentin bonding as a function of dentin structure.," *Dental clinics of North America*. 2002.

[22] E. W. Neuse and E. Mizrahi, "Bonding Materials and Techniques in Dentistry," in *Handbook of Adhesive Technology*, 2d edition., A. Pizzi and K. L. Mittal, Eds. Marcel Dekker, Inc, 2003.

[23] N. Nakabayashi, M. Nakamura, and N. Yasuda, "Hybrid Layer as a Dentin-Bonding Mechanism," *J. Esthet. Restor. Dent.*, 1991.

[24] N. Nakabayashi, K. Kojima, and E. Masuhara, "The promotion of adhesion by the infiltration of monomers into tooth substrates," *J. Biomed. Mater. Res.*, 1982.

[25] P. C. V. Yamazaki, A. K. B. Bedran-Russo, and P. N. R. Pereira, "Importance of the hybrid layer on the bond strength of restorations subjected to cyclic loading," *Journal of Biomedical Materials Research - Part B Applied Biomaterials*. 2008.

[26] A. Sezinando, "Looking for the ideal adhesive - A review," *Revista Portuguesa de Estomatologia, Medicina Dentaria e Cirurgia Maxilofacial*. 2014.

[27] P. Spencer, Q. Ye, J. Park, A. Misra, B. S. Bohaty, V. Singh, R. Parthasarathy, F. Sene, S. Gonçalves, and J. Laurence, “Durable Bonds at the Adhesive/Dentin Interface: An Impossible Mission or Simply a Moving Target?,” *Brazilian Dent. Sci.*, 2012.

[28] N. Dunne and C. Mitchell, “Biomedical/bioengineering applications of carbon nanotube-based nanocomposites,” in *Polymer-Carbon Nanotube Composites: Preparation, Properties and Applications*, 2011.

[29] J. Perdigão, S. Duarte, and G. Gomes, “Direct resin-based composite restorations - Clinical challenges,” in *Adhesion Aspects in Dentristry*, J. P. Matinlinna and K. L. Mittal, Eds. VSP, 2009, p. pp.35-48.

[30] A. Takahashi, Y. Sato, S. Uno, P. N. R. Pereira, and H. Sano, “Effects of mechanical properties of adhesive resins on bond strength to dentin,” *Dent. Mater.*, 2002.

[31] K. L. Van Landuyt, J. Snauwaert, J. De Munck, M. Peumans, Y. Yoshida, A. Poitevin, E. Coutinho, K. Suzuki, P. Lambrechts, and B. Van Meerbeek, “Systematic review of the chemical composition of contemporary dental adhesives,” *Biomaterials*, vol. 28, no. 26. pp. 3757–3785, 2007.

[32] H. Sano, N. Kanemura, M. F. Burrow, N. Inai, T. Yamada, and J. Tagami, “Effect of operator variability on dentin adhesion: students vs. dentists,” *Dent. Mater. J.*, 1998.

[33] E. Milia, E. Cumbo, R. Jose A. Cardoso, and G. Gallina, “Current Dental Adhesives Systems. A Narrative Review,” *Curr. Pharm. Des.*, 2012.

[34] F. A. Rueggeberg, M. Giannini, C. A. G. Arrais, and R. B. T. Price, “Light curing in dentistry and clinical implications: a literature review,” *Braz. Oral Res.*, vol. 31, no. suppl 1, 2017.

[35] K. L. Van Landuyt, J. Snauwaert, M. Peumans, J. De Munck, P. Lambrechts, and B. Van Meerbeek, “The role of HEMA in one-step self-etch adhesives,” *Dent. Mater.*, 2008.

[36] D. Horak, A. Jayakrishnan, and A. Arshady, “Poly(2-hydroxyethyl methacrylate) Hydrogels: preparation and Properties,” in *Introduction to polymeric biomaterials*, Citus Books, London, 2003, pp. 65–99.

[37] K. Aalto-Korte, K. Alanko, O. Kuuliala, and R. Jolanki, “Methacrylate and acrylate allergy in dental personnel,” *Contact Dermatitis*, 2007.

[38] H.-N. Lim, S.-H. Kim, B. Yu, and Y.-K. Lee, “Influence of HEMA content on the mechanical and bonding properties of experimental HEMA-added glass

ionomer cements.," *J. Appl. Oral Sci.*, 2009.

[39] W. Geurtsen and G. Leyhausen, "Concise Review Biomaterials & Bioengineering: Chemical-Biological Interactions of the Resin Monomer Triethyleneglycol-dimethacrylate (TEGDMA)," *J. Dent. Res.*, 2001.

[40] I. D. Sideridou, M. M. Karabela, and E. C. Vouvoudi, "Dynamic thermomechanical properties and sorption characteristics of two commercial light cured dental resin composites," *Dent. Mater.*, 2008.

[41] S. H. Dickens, J. W. Stansbury, K. M. Choi, and C. J. E. Floyd, "Photopolymerization kinetics of methacrylate dental resins," *Macromolecules*, 2003.

[42] W. F. Schroeder and C. I. Vallo, "Effect of different photoinitiator systems on conversion profiles of a model unfilled light-cured resin," *Dent. Mater.*, 2007.

[43] Y. Imai, Y. Kadoma, K. Kojima, T. Akimoto, K. Ikakura, and T. Ohta, "Importance of Polymerization Initiator Systems and Interfacial Initiation of Polymerization in Adhesive Bonding of Resin to Dentin," *J. Dent. Res.*, 1991.

[44] E. A. Kamoun, A. Winkel, M. Eisenburger, and H. Menzel, "Carboxylated camphorquinone as visible-light photoinitiator for biomedical application: Synthesis, characterization, and application Carboxylated camphorquinone as visible-light photoinitiator," *Arab. J. Chem.*, 2016.

[45] W. Y. Tseng, C. H. Huang, R. S. Chen, M. S. Lee, Y. J. Chen, F. A. Rueggeberg, and M. H. Chen, "Monomer conversion and cytotoxicity of dental composites irradiated with different modes of photoactivated curing," *J. Biomed. Mater. Res. - Part B Appl. Biomater.*, 2007.

[46] T. Atsumi, M. Ishihara, Y. Kadoma, K. Tonosaki, and S. Fujisawa, "Comparative radical production and cytotoxicity induced by camphorquinone and 9-fluorenone against human pulp fibroblasts," *J. Oral Rehabil.*, 2004.

[47] J. Jakubiak, X. Allonas, J. P. Fouassier, A. Sionkowska, E. Andrzejewska, L. Å. Linden, and J. F. Rabek, "Camphorquinone-amines photoinitating systems for the initiation of free radical polymerization," *Polymer (Guildf).*, 2003.

[48] J. D. Oxman, D. W. Jacobs, M. C. Trom, V. Sipani, B. Ficek, and A. B. Scranton, "Evaluation of initiator systems for controlled and sequentially curable free-radical/cationic hybrid photopolymerizations," *J. Polym. Sci. Part A Polym. Chem.*, 2005.

[49] A. Ogunyinka, W. M. Palin, A. C. Shortall, and P. M. Marquis, "Photoinitiation chemistry affects light transmission and degree of conversion of curing

experimental dental resin composites," *Dent. Mater.*, 2007.

[50] X. Guo, Y. Wang, P. Spencer, Q. Ye, and X. Yao, "Effects of water content and initiator composition on photopolymerization of a model BisGMA/HEMA resin," *Dent. Mater.*, 2008.

[51] J. Park, Q. Ye, E. M. Topp, A. Misra, S. L. Kieweg, and P. Spencer, "Effect of photoinitiator system and water content on dynamic mechanical properties of a light-cured bisGMA/HEMA dental resin," *J. Biomed. Mater. Res. - Part A*, 2010.

[52] X. Guo, Z. Peng, P. Spencer, and Y. Wang, "Effect of initiator on photopolymerization of acidic, aqueous dental model adhesives," *J. Biomed. Mater. Res. - Part A*, 2009.

[53] L. Song, Q. Ye, X. Ge, A. Misra, and P. Spencer, "Tris(trimethylsilyl)silane as a co-initiator for dental adhesive: Photo-polymerization kinetics and dynamic mechanical property.," *Dent. Mater.*, 2016.

[54] M. Ali Tehfe, M. El-Roz, J. Lalevée, F. Morlet-Savary, B. Graff, and J. P. Fouassier, "Bifunctional co-initiators: A new strategy for the design of efficient systems in radical photopolymerization reactions under air," *Eur. Polym. J.*, 2012.

[55] K. Ikemura and T. Endo, "A Review of our Development of Dental Adhesives-Effects of Radical Polymerization Initiators and Adhesive Monomers on Adhesion.," *Dent. Mater. J.*, 2010.

[56] N. B. Cramer, J. W. Stansbury, and C. N. Bowman, "Recent advances and developments in composite dental restorative materials," in *Journal of Dental Research*, 2011.

[57] T. Jacobsen and K. J. Söderholm, "Some effects of water on dentin bonding," *Dent. Mater.*, 1995.

[58] M. H. Silva E Souza, K. G. K. Carneiro, M. F. Lobato, P. D. A. R. Silva E Souza, and M. F. De Góes, "Adhesive systems: important aspects related to their composition and clinical use.," *J. Appl. oral Sci. Rev. FOB*, 2010.

[59] S. H. Kasraei, M. Atai, Z. Khamverdi, and S. K. Nejad, "Effect of Nanofiller Addition to an Experimental Dentin Adhesive on Microtensile Bond Strength to Human Dentin," *Sci. York*, 2009.

[60] A. Wagner, R. Belli, C. Stötzel, A. Hilpert, F. A. Müller, and U. Lohbauer, "Biomimetically- and hydrothermally-grown HAp nanoparticles as reinforcing fillers for dental adhesives.," *J. Adhes. Dent.*, 2013.

[61] G. Baaran, T. Özer, and J. Deveciolu Kama, “Comparison of a recently developed nanofiller self-etching primer adhesive with other self-etching primers and conventional acid etching,” *Eur. J. Orthod.*, 2009.

[62] A. Dufresne, “Nanocellulose: A new ageless bionanomaterial,” *Mater. Today*, 2013.

[63] Y. Habibi, L. A. Lucia, and O. J. Rojas, “Cellulose nanocrystals: Chemistry, self-assembly, and applications,” *Chem. Rev.*, 2010.

[64] D. Klemm, F. Kramer, S. Moritz, T. Lindström, M. Ankerfors, D. Gray, and A. Dorris, “Nanocelluloses: A new family of nature-based materials,” *Angewandte Chemie - International Edition*. 2011.

[65] M. Jonoobi, R. Oladi, Y. Davoudpour, K. Oksman, A. Dufresne, Y. Hamzeh, and R. Davoodi, “Different preparation methods and properties of nanostructured cellulose from various natural resources and residues: a review,” *Cellulose*. 2015.

[66] S. Elazzouzi-Hafraoui, Y. Nishiyama, J. L. Putaux, L. Heux, F. Dubreuil, and C. Rochas, “The shape and size distribution of crystalline nanoparticles prepared by acid hydrolysis of native cellulose,” *Biomacromolecules*, 2008.

[67] M. Mariano, N. El Kissi, and A. Dufresne, “Cellulose nanocrystals and related nanocomposites: Review of some properties and challenges,” *Journal of Polymer Science, Part B: Polymer Physics*. 2014.

[68] N. Lin, J. Huang, and A. Dufresne, “Preparation, properties and applications of polysaccharide nanocrystals in advanced functional nanomaterials: A review,” *Nanoscale*. 2012.

[69] C. Miao and W. Y. Hamad, “Cellulose reinforced polymer composites and nanocomposites: A critical review,” *Cellulose*. 2013.

[70] E. Kontturi, P. Laaksonen, M. B. Linder, Nonappa, A. H. Gröschel, O. J. Rojas, and O. Ikkala, “Advanced Materials through Assembly of Nanocelluloses,” *Advanced Materials*. 2018.

[71] H. Y. Yu, R. Chen, G. Y. Chen, L. Liu, X. G. Yang, and J. M. Yao, “Silylation of cellulose nanocrystals and their reinforcement of commercial silicone rubber,” *J. Nanoparticle Res.*, 2015.

[72] X. Xu, F. Liu, L. Jiang, J. Y. Zhu, D. Haagenson, and D. P. Wiesenborn, “Cellulose nanocrystals vs. Cellulose nanofibrils: A comparative study on their microstructures and effects as polymer reinforcing agents,” *ACS Appl. Mater. Interfaces*, 2013.

[73] X. Cao, Y. Habibi, and L. A. Lucia, “One-pot polymerization, surface grafting, and processing of waterborne polyurethane-cellulose nanocrystal nanocomposites,” *J. Mater. Chem.*, 2009.

[74] P. Pooyan, R. Tannenbaum, and H. Garmestani, “Mechanical behavior of a cellulose-reinforced scaffold in vascular tissue engineering,” *J. Mech. Behav. Biomed. Mater.*, 2012.

[75] W. P. Flauzino Neto, M. Mariano, I. S. V. da Silva, H. A. Silvério, J. L. Putaux, H. Otaguro, D. Pasquini, and A. Dufresne, “Mechanical properties of natural rubber nanocomposites reinforced with high aspect ratio cellulose nanocrystals isolated from soy hulls,” *Carbohydr. Polym.*, 2016.

[76] I. Sakurada, Y. Nukushina, and T. Ito, “Experimental determination of the elastic modulus of crystalline regions oriented polymers,” *J. Polym. Sci.*, 1962.

[77] R. J. Moon, A. Martini, J. Nairn, J. Simonsen, and J. Youngblood, “Cellulose nanomaterials review: Structure, properties and nanocomposites,” *Chemical Society Reviews*. 2011.

[78] R. M. Silva, F. V. Pereira, F. A. P. Mota, E. Watanabe, S. M. C. S. Soares, and M. H. Santos, “Dental glass ionomer cement reinforced by cellulose microfibers and cellulose nanocrystals,” *Mater. Sci. Eng. C*, 2016.

[79] R. Menezes-Silva, F. V. Pereira, M. H. Santos, J. A. Soares, S. M. C. S. Soares, and J. L. De Miranda, “Biocompatibility of a new dental glass ionomer cement with cellulose microfibers and cellulose nanocrystals,” *Braz. Dent. J.*, 2017.

[80] T. Pääkkönen, P. Spiliopoulos, A. Knuts, K. Nieminen, L.-S. Johansson, E. Enqvist, and E. Kontturi, “From vapour to gas: optimising cellulose degradation with gaseous HCl,” *React. Chem. Eng.*, 2018.

[81] S. Camarero Espinosa, T. Kuhnt, E. J. Foster, and C. Weder, “Isolation of thermally stable cellulose nanocrystals by phosphoric acid hydrolysis,” *Biomacromolecules*, vol. 14, no. 4, pp. 1223–1230, 2013.

[82] O. M. Vanderfleet, D. A. Osorio, and E. D. Cranston, “Optimization of cellulose nanocrystal length and surface charge density through phosphoric acid hydrolysis.,” *Philos. Trans. A. Math. Phys. Eng. Sci.*, 2018.

[83] P. L. Granja, L. Pouysgu, M. Ptraud, B. De Jso, C. Baquey, and M. A. Barbosa, “Cellulose phosphates as biomaterials. I. Synthesis and characterization of highly phosphorylated cellulose gels,” *J. Appl. Polym. Sci.*,

2001.

[84] Y. Habibi, L. A. Lucia, and O. J. Rojas, “Cellulose nanocrystals: Chemistry, self-assembly, and applications,” *Chem. Rev.*, vol. 110, no. 6, pp. 3479–3500, 2010.

[85] J. P. Matinlinna, L. V. J. Lassila, M. Ozcan, A. Yli-Urpo, and P. K. Vallittu, “An introduction to silanes and their clinical applications in dentistry.,” *Int. J. Prosthodont.*, 2004.

[86] J. P. Matinlinna, C. Y. K. Lung, and J. K. H. Tsoi, “Silane adhesion mechanism in dental applications and surface treatments: A review,” *Dental Materials*. 2018.

[87] Y. Xie, C. A. S. Hill, Z. Xiao, H. Militz, and C. Mai, “Silane coupling agents used for natural fiber/polymer composites: A review,” *Composites Part A: Applied Science and Manufacturing*. 2010.

[88] M. Abdelmouleh, S. Boufi, A. Ben Salah, M. N. Belgacem, and A. Gandini, “Interaction of silane coupling agents with cellulose,” *Langmuir*, vol. 18, no. 8, pp. 3203–3208, 2002.

[89] R. M. Sheltami, H. Kargarzadeh, and I. Abdullah, “Effects of silane surface treatment of cellulose nanocrystals on the tensile properties of cellulose-polyvinyl chloride nanocomposite,” *Sains Malaysiana*, 2015.

[90] C. Goussé, H. Chanzy, G. Excoffier, L. Soubeyrand, and E. Fleury, “Stable suspensions of partially silylated cellulose whiskers dispersed in organic solvents,” *Polymer (Guildf).*, vol. 43, no. 9, pp. 2645–2651, 2002.

[91] M. Beaumont, M. Bacher, M. Opietnik, W. Gindl-Altmutter, A. Potthast, and T. Rosenau, “A general aqueous silanization protocol to introduce vinyl, mercapto or azido functionalities onto cellulose fibers and nanocelluloses,” *Molecules*, 2018.

[92] M. Fumagalli, D. Ouhab, S. M. Boisseau, and L. Heux, “Versatile gas-phase reactions for surface to bulk esterification of cellulose microfibrils aerogels,” *Biomacromolecules*, vol. 14, no. 9, pp. 3246–3255, 2013.

[93] S. Berlioz, S. Molina-Boisseau, Y. Nishiyama, and L. Heux, “Gas-phase surface esterification of cellulose microfibrils and whiskers,” *Biomacromolecules*, vol. 10, no. 8, pp. 2144–2151, 2009.

[94] X. M. Dong, J.-F. Revol, and D. G. Gray, “Effect of microcrystallite preparation conditions on the formation of colloid crystals of cellulose,” *Cellulose*, vol. 5, pp. 19–32, 1998.

[95] E. Kontturi, L. S. Johansson, K. S. Kontturi, P. Ahonen, P. C. Thüne, and J. Laine, “Cellulose nanocrystal submonolayers by spin coating,” *Langmuir*, vol. 23, no. 19, pp. 9674–9680, 2007.

[96] R. Salminen, N. Baccile, M. Reza, and E. Kontturi, “Surface-Induced Frustration in Solid State Polymorphic Transition of Native Cellulose Nanocrystals,” *Biomacromolecules*, 2017.

[97] A. W. T. King, V. Mäkelä, S. A. Kedzior, T. Laaksonen, G. J. Partl, S. Heikkinen, H. Koskela, H. A. Heikkinen, A. J. Holding, E. D. Cranston, and I. Kilpeläinen, “Liquid-State NMR Analysis of Nanocelluloses,” *Biomacromolecules*, 2018.

[98] S. Imazato, J. F. McCabe, H. Tarumi, A. Ehara, and S. Ebisu, “Degree of conversion of composites measured by DTA and FTIR,” *Dent. Mater.*, 2001.

[99] G. J. Pearson and C. M. Longman, “Water sorption and solubility of resin-based materials following inadequate polymerization by a visible-light curing system,” *J. Oral Rehabil.*, vol. 16, no. 1, pp. 57–61, 1989.

[100] F. A. Rueggeberg, D. T. Hashinger, and C. W. Fairhurst, “Calibration of FTIR conversion analysis of contemporary dental resin composites,” *Dent. Mater.*, 1990.

[101] ISO 40449:2009 (E), *International Standard Iso*, vol. 2006. 2006.

[102] S. M. Chung, A. U. J. Yap, S. P. Chandra, and C. T. Lim, “Flexural strength of dental composite restoratives: Comparison of biaxial and three-point bending test,” *J. Biomed. Mater. Res. - Part B Appl. Biomater.*, 2004.

[103] M. Labet and W. Thielemans, “Improving the reproducibility of chemical reactions on the surface of cellulose nanocrystals: ROP of ε-caprolactone as a case study,” *Cellulose*, 2011.

[104] E. J. Foster, R. J. Moon, U. P. Agarwal, M. J. Bortner, J. Bras, S. Camarero-Espinosa, K. J. Chan, M. J. D. Clift, E. D. Cranston, S. J. Eichhorn, D. M. Fox, W. Y. Hamad, L. Heux, B. Jean, M. Korey, W. Nieh, K. J. Ong, M. S. Reid, S. Renneckar, R. Roberts, J. A. Shatkin, J. Simonsen, K. Stinson-Bagby, N. Wanasekara, and J. Youngblood, “Current characterization methods for cellulose nanomaterials,” *Chemical Society Reviews*. 2018.

[105] S. Eyley and W. Thielemans, “Surface modification of cellulose nanocrystals,” *Nanoscale*, vol. 6, no. 14, pp. 7764–7779, 2014.

[106] S. Beck, M. Méthot, and J. Bouchard, “General procedure for determining cellulose nanocrystal sulfate half-ester content by conductometric titration,”

Cellulose, 2015.

[107] M. S. Reid, M. Villalobos, and E. D. Cranston, “Benchmarking Cellulose Nanocrystals: From the Laboratory to Industrial Production,” *Langmuir*. 2017.

[108] H.-F. Klein, “Practical Interpretation of P-31 NMR Spectra and Computer Assisted Structure Verification. Von Louis D. Quin und Antony J. Williams.,” *Angew. Chemie Int. Ed.*, 2005.

[109] M. Abdelmouleh, S. Boufi, M. N. Belgacem, A. P. Duarte, A. Ben Salah, and A. Gandini, “Modification of cellulosic fibres with functionalised silanes: Development of surface properties,” *Int. J. Adhes. Adhes.*, 2004.

[110] M. Abdelmouleh, S. Boufi, M. N. Belgacem, and A. Dufresne, “Short natural-fibre reinforced polyethylene and natural rubber composites: Effect of silane coupling agents and fibres loading,” *Compos. Sci. Technol.*, 2007.

[111] M. Tian, Y. Gao, Y. Liu, Y. Liao, N. E. Hedin, and H. Fong, “Fabrication and evaluation of Bis-GMA/TEGDMA dental resins/composites containing nano fibrillar silicate,” *Dent. Mater.*, 2008.

[112] W. M. Palin, G. J. P. Fleming, F. J. Trevor Burke, P. M. Marquis, and R. C. Randall, “The reliability in flexural strength testing of a novel dental composite,” *J. Dent.*, vol. 31, no. 8, pp. 549–557, 2003.

[113] W. M. Palin, G. J. P. Fleming, and P. M. Marquis, “The reliability of standardized flexure strength testing procedures for a light-activated resin-based composite,” *Dental Materials*. 2005.

[114] D. Miura, T. Miyasaka, H. Aoki, Y. Aoyagi, and Y. Ishida, “Correlations among bending test methods for dental hard resins,” *Dent. Mater. J.*, vol. 36, no. 4, pp. 491–496, 2017.

[115] S. A. Jivraj, T. H. Kim, and T. E. Donovan, “Selection of luting agents, part 1,” *J Calif Dent Assoc*, 2006.

[116] D. Bondeson and K. Oksman, “Polylactic acid/cellulose whisker nanocomposites modified by polyvinyl alcohol,” *Compos. Part A Appl. Sci. Manuf.*, 2007.

[117] Y. W. Chen, T. H. Tan, H. V. Lee, and S. B. A. Hamid, “Easy fabrication of highly thermal-stable cellulose nanocrystals using Cr(NO3)3catalytic hydrolysis system: A feasibility study from macroto nano-dimensions,” *Materials (Basel).*, 2017.

[118] B. L. Peng, N. Dhar, H. L. Liu, and K. C. Tam, “Chemistry and applications of nanocrystalline cellulose and its derivatives: A nanotechnology perspective,”

Canadian Journal of Chemical Engineering. 2011.

[119] V. Khoshkava and M. R. Kamal, “Effect of drying conditions on cellulose nanocrystal (CNC) agglomerate porosity and dispersibility in polymer nanocomposites,” *Powder Technol.*, 2014.

[120] J. Sapkota, J. C. Martinez Garcia, and M. Lattuada, “Reinterpretation of the mechanical reinforcement of polymer nanocomposites reinforced with cellulose nanorods,” *J. Appl. Polym. Sci.*, 2017.

[121] S. J. Eichhorn, “Cellulose nanowhiskers: Promising materials for advanced applications,” *Soft Matter*. 2011.

[122] I. Kalashnikova, H. Bizot, P. Bertoncini, B. Cathala, and I. Capron, “Cellulosic nanorods of various aspect ratios for oil in water Pickering emulsions,” *Soft Matter*, 2013.

Appendices

APPENDIX 1

Table A1. Flexural strength test results for the nanocomposites (HEMA/TEGDMA

Sample	Height (mm)	Width (mm)	Maximum Load (N)	Maximum Deflection (mm)	The flexural strength, (MPa)	Young's Modulus of Bending (MPa)
Reference 1	1,60	1,95	4,22	5,35	25,38	556,26
Reference 2	2,35	1,95	10,15	5,30	28,28	725,95
Reference 3	2,41	1,95	8,78	6,00	23,25	653,36
Reference 4	2,01	1,95	6,49	5,08	24,73	804,21
Reference 5	2,67	1,94	18,37	4,41	39,85	865,57
Mean value	**2,21**	**1,95**	**9,60**	**5,23**	**28,30**	**721,07**
Standard deviation	**0,41**	**0,00**	**5,40**	**0,57**	**6,71**	**122,03**
PCNC 3 wt.% 1	1,84	1,98	4,92	3,87	22,00	649,76
PCNC 3 wt.% 2	1,75	1,92	5,43	5,39	27,69	805,26
PCNC 3 wt.% 3	1,60	1,95	3,60	5,39	21,64	494,28
PCNC 3 wt.% 4	1,90	1,94	9,61	4,38	41,17	1370,39
PCNC 3 wt.% 5	1,40	1,95	2,23	5,06	17,49	470,36
Mean value	**1,65**	**1,95**	**4,51**	**4,61**	**26,00**	**681,91**
Standard deviation	**0,22**	**0,02**	**2,95**	**0,79**	**10,49**	**378,15**
PCNC 5 wt.% 1	2,15	1,95	11,06	2,94	36,80	906,32
PCNC 5 wt.% 2	1,98	1,95	4,78	3,99	18,74	419,68
PCNC 5 wt.% 3	1,96	1,95	10,57	4,61	42,35	1077,45
PCNC 5 wt.% 4	2,04	1,95	12,21	4,71	45,15	1077,38
PCNC 5 wt.% 5	1,80	1,95	4,85	4,16	23,05	529,60
PCNC 5 wt.% 6	1,45	1,95	3,32	5,91	24,33	572,04
Mean value	**1,90**	**1,95**	**7,80**	**4,39**	**31,74**	**763,74**
Standard deviation	**0,25**	**0,00**	**3,89**	**0,98**	**11,11**	**292,25**
PCNC 7 wt.% 1	1,9	2,0	2,3	4,3	9,6	227,8
PCNC 7 wt.% 2	1,8	2,0	2,9	5,3	13,4	315,9
PCNC 7 wt.% 3	1,7	2,0	2,4	3,4	12,9	271,7
Mean value	**1,73**	**1,95**	**2,03**	**4,73**	**9,88**	**222,66**
Standard deviation	**0,19**	**0,00**	**1,05**	**1,14**	**4,58**	**104,68**
mPCNC2 1 wt.% 1	1,92	1,95	2,31	4,29	9,64	227,75
mPCNC2 1 wt.% 2	1,81	1,95	2,86	5,25	13,43	315,94
mPCNC2 1 wt.% 3	1,70	1,95	2,43	3,39	12,95	271,74
mPCNC2 1 wt.% 4	1,79	1,95	3,67	4,61	17,64	383,30
Mean value	**1,86**	**1,94**	**2,98**	**3,59**	**13,67**	**368,46**
Standard	**0,19**	**0,01**	**1,17**	**1,55**	**5,75**	**101,20**

deviation						
mPCNC2 3 wt.% 1	2,01	1,95	4,33	4,12	16,47	390,03
mPCNC2 3 wt.% 2	1,94	1,95	2,50	5,16	10,24	225,97
mPCNC2 3 wt.% 3	1,91	1,95	3,64	5,59	15,35	441,72
mPCNC2 3 wt.% 4	1,82	1,95	2,76	3,93	12,84	328,28
mPCNC2 3 wt.% 5	1,80	1,95	2,63	5,18	12,49	304,52
mPCNC2 3 wt.% 6	1,80	1,95	2,37	3,72	11,23	231,13
Mean value	**1,88**	**1,95**	**3,04**	**4,62**	**13,10**	**320,27**
Standard deviation	**0,09**	**0,00**	**0,77**	**0,79**	**2,39**	**85,75**
mPCNC2 5 wt.% 1	1,67	1,94	0,45	6,00	2,52	45508,45
mPCNC2 5 wt.% 2	1,89	1,94	0,77	6,00	3,33	147,24
mPCNC2 5 wt.% 3	1,60	1,94	1,08	3,65	6,52	177,24
Mean value	**1,72**	**1,94**	**0,77**	**5,22**	**4,12**	**15277,64**
Standard deviation	**0,15**	**0,00**	**0,31**	**1,36**	**2,12**	**26180,65**

Table A2. Flexural strength test results for the nanocomposites (bisGMA/TEGDMA)

Sample	**Height (mm)**	**Width (mm)**	**Maximum Load (N)**	**Maximum Deflection (mm)**	**Maximum Bending Stress at Maximum Load (MPa)**	**Young's Modulus of Bending (MPa)**
Reference 1	1,85	1,87	17,23	1,41	80,76	2357,11
Reference 2	1,98	1,87	24,42	2,27	99,92	2278,98
Reference 3	1,91	1,87	22,66	2,47	99,65	2162,37
Reference 4	1,95	1,87	21,42	1,79	90,36	2113,23
Reference 5	2,01	1,87	14,46	0,98	57,44	2295,68
Reference 6	1,91	1,87	21,65	2,34	95,20	2326,58
Mean value	**1,94**	**1,87**	**20,31**	**1,88**	**87,22**	**2255,66**
Standard deviation	**0,06**	**0,00**	**3,72**	**0,59**	**16,24**	**96,39**
PCNC 1 wt.% 1	1,93	1,87	19,63	1,65	84,53	2169,93
PCNC 1 wt.% 2	1,98	1,87	14,87	1,14	60,85	2007,44
PCNC 1 wt.% 3	1,95	1,87	20,03	1,63	84,52	2094,48
PCNC 1 wt.% 4	2,02	1,87	12,16	0,86	47,80	2016,28
PCNC 1 wt.% 5	1,93	1,87	13,26	1,06	57,11	2047,18
PCNC 1 wt.% 6	1,94	1,87	19,04	1,53	81,16	2149,85
Mean value	**1,96**	**1,87**	**16,50**	**1,31**	**69,33**	**2080,86**
Standard deviation	**0,04**	**0,00**	**3,49**	**0,33**	**16,04**	**68,67**
PCNC 3 wt.% 1	1,88	1,87	13,04	1,03	59,17	2253,96
PCNC 3 wt.% 2	1,95	1,87	15,41	1,06	65,03	2366,88

PCNC 3 wt.% 3	1,95	1,87	17,03	1,05	71,84	2606,03
PCNC 3 wt.% 4	1,96	1,87	18,89	1,29	78,90	2493,93
PCNC 3 wt.% 5	1,93	1,87	18,80	1,33	80,99	2566,70
PCNC 3 wt.% 6	1,98	1,87	18,24	1,16	74,65	2410,88
Mean value	**1,94**	**1,87**	**16,90**	**1,15**	**71,76**	**2449,73**
Standard deviation	**0,03**	**0,00**	**2,31**	**0,13**	**8,35**	**131,73**
mPCNC2 1 wt.% 1	2,01	1,91	11,66	0,89	45,34	1936,91
mPCNC2 1 wt.% 2	1,98	1,91	15,96	1,23	63,96	1987,12
mPCNC2 1 wt.% 3	2,03	1,91	13,39	1,01	51,02	1833,62
mPCNC2 1 wt.% 4	2,03	1,91	19,68	1,54	75,03	1985,44
mPCNC2 1 wt.% 5	2,05	1,91	15,56	1,04	58,16	1994,29
mPCNC2 1 wt.% 6	2,05	1,91	19,29	1,43	72,11	1856,56
Mean value	**2,03**	**1,91**	**15,93**	**1,19**	**60,94**	**1932,32**
Standard deviation	**0,03**	**0,00**	**3,17**	**0,26**	**11,68**	**70,95**
mPCNC2 3wt.% 1	1,99	1,91	16,83	1,23	66,77	2068,17
mPCNC2 3wt.% 2	1,98	1,91	14,24	1,03	57,05	2123,17
mPCNC2 3wt.% 3	2,00	1,91	15,08	1,16	59,20	1903,36
mPCNC2 3wt.% 4	2,01	1,91	6,85	0,49	26,63	1918,34
mPCNC2 3wt.% 5	2,01	1,91	10,24	0,73	39,82	1911,70
mPCNC2 3wt.% 6	2,04	1,91	16,28	0,96	61,45	2420,28
Mean value	**2,01**	**1,91**	**13,25**	**0,93**	**51,82**	**2057,50**
Standard deviation	**0,02**	**0,00**	**3,91**	**0,28**	**15,34**	**200,21**

APPENDIX 2

a)

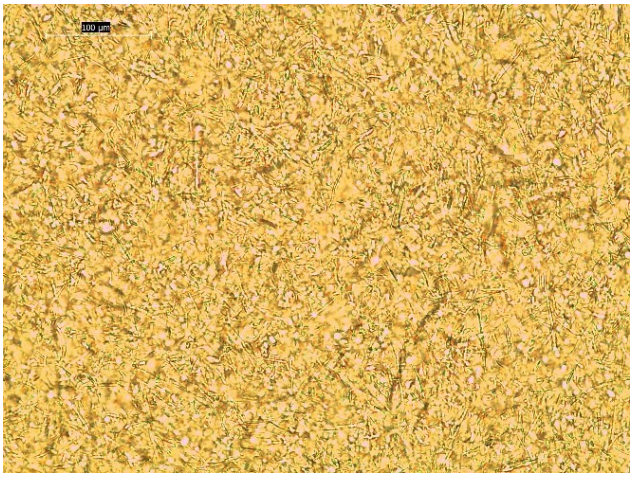

b)

c)

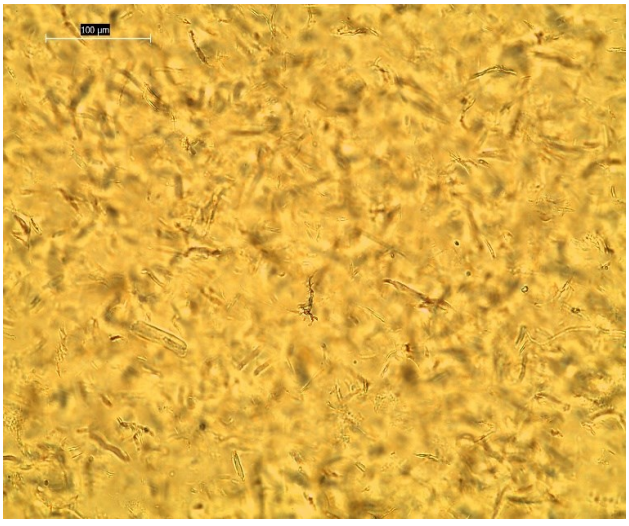

Figure A1. Light microscopy images of liquid unpolymerized nanocomposites: a) 3 wt.% mPCNC2 in HEMA/TEGDMA b) 3 wt.% mPCNC2 in bisGMA/TEGDMA and c) 3 wt.% PCNC in bisGMA/TEGDMA